Member of the Helmholtz Association

TRILATERAL
EUREGIO CLUSTER

JÜLICH
FORSCHUNGSZENTRUM

Behavior of tungsten under thermal and plasma exposure and development of advanced tungsten materials

M. Wirtz, M. Berger, L. Buzi, J. Coenen, A. Huber, A. Kreter, N. Lemahieu, B. Jaspers, J. Linke, A. Litnovsky, D. Matveev, G. Pintsuk, M. Rasinski, M. Reinhart, G. Sergienko, I. Steudel, T. Wegener, B. Unterberg

Forschungszentrum Jülich GmbH, Institute of Energy and Climate Research, 52425 Jülich, Germany

3nd RCM on PWI with irradiated Tungsten and Tungsten Alloys in Fusion Devices,
27 - 30 June 2017, Vienna, Austria

Outline of FZJ contributions

- Thermal shock behavior of irradiated and un-irradiated W grades
- Change of W micro- structure under simultaneous heat and particle loads and impact on W erosion and fuel retention in W
- Development of advanced tungsten materials with improved micro-structure
- Characterization of commercially available tungsten grades

A

Environmental conditions - test facilities

Environmental conditions

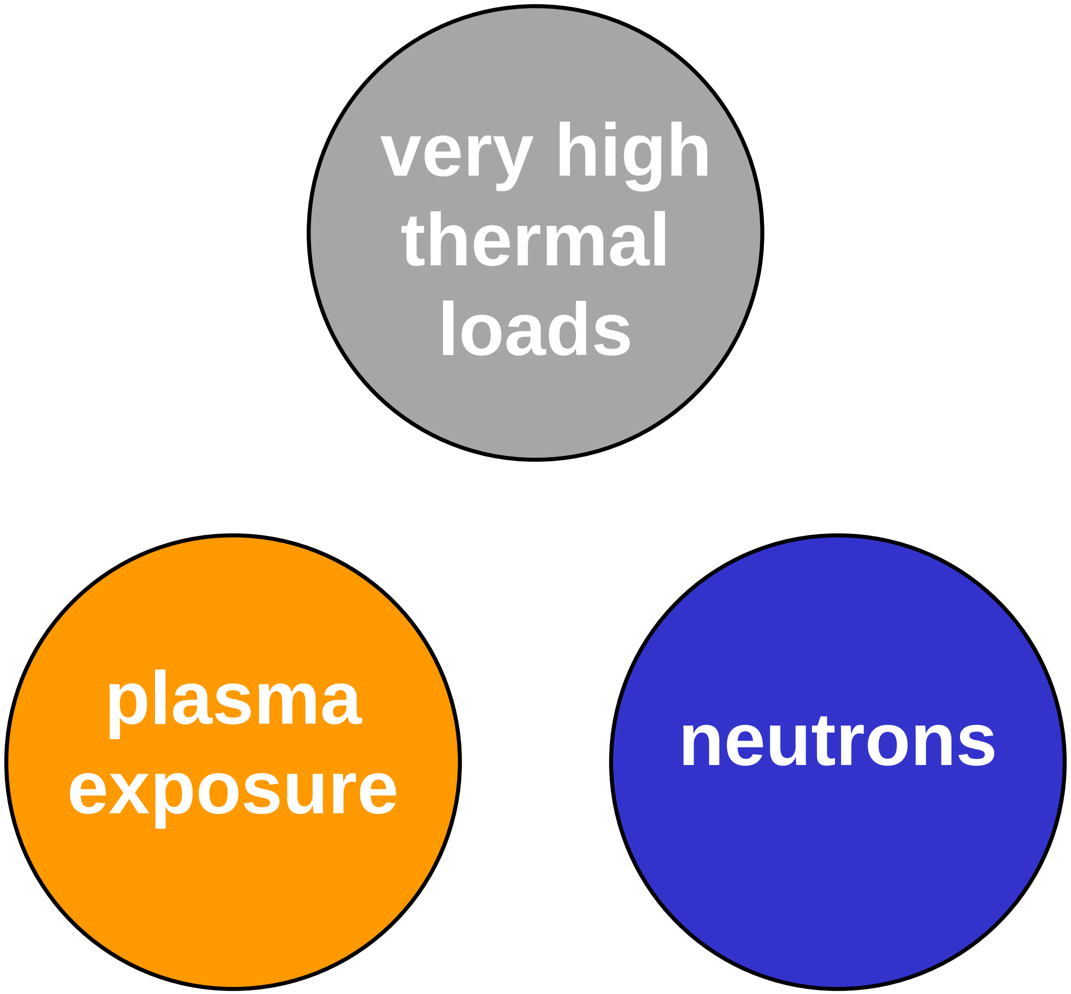

Environmental conditions

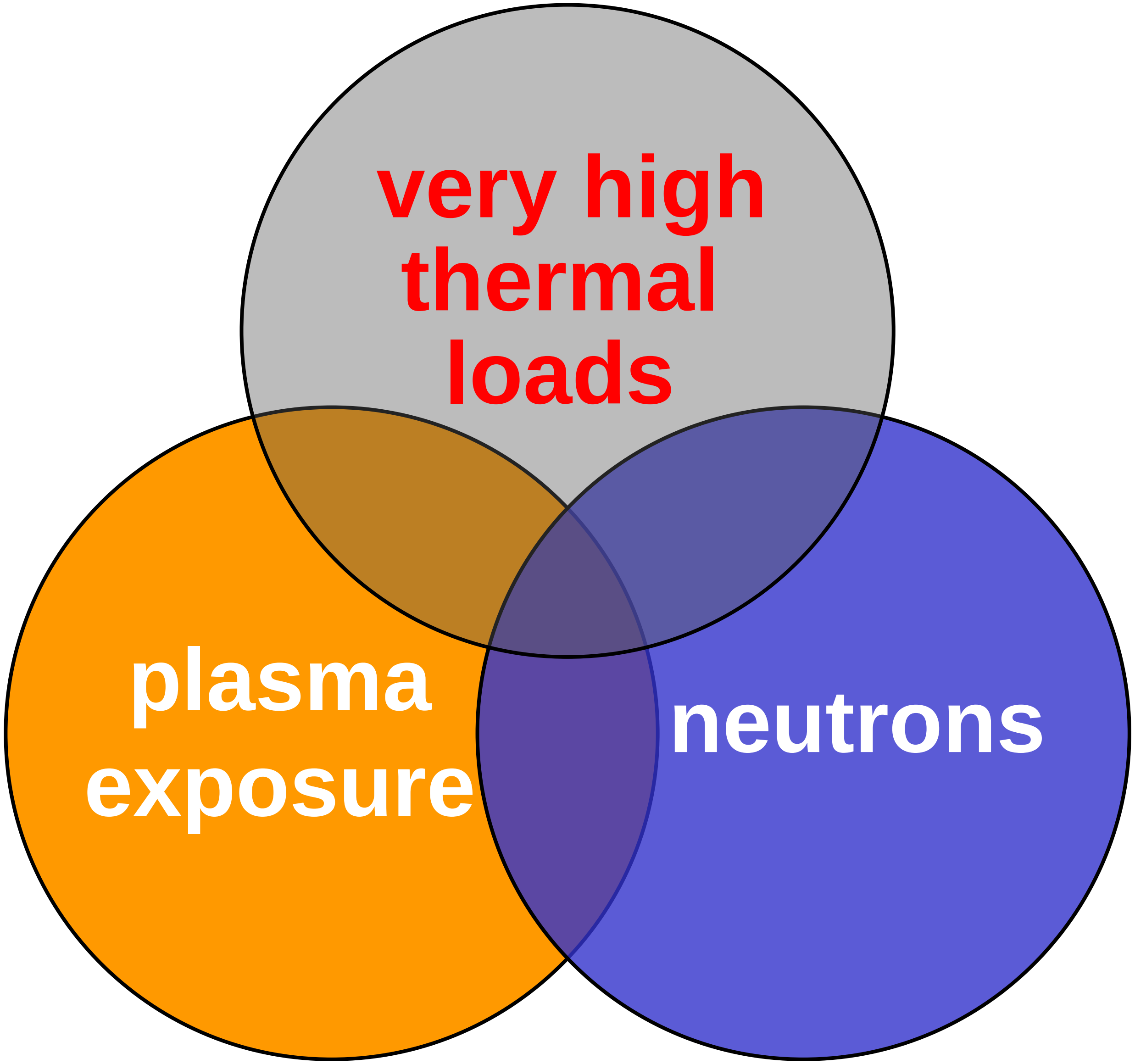

Environmental conditions

Steady state heat loads:

up to 20 MWm^{-2} in ITER
(lower loads in DEMO)

- recrystallization
- failure of joints

Transient thermal loads:

up to 60 MJm^{-2}
(disrupt., ELMs, VDEs)

- crackings
- melting
- dust formation

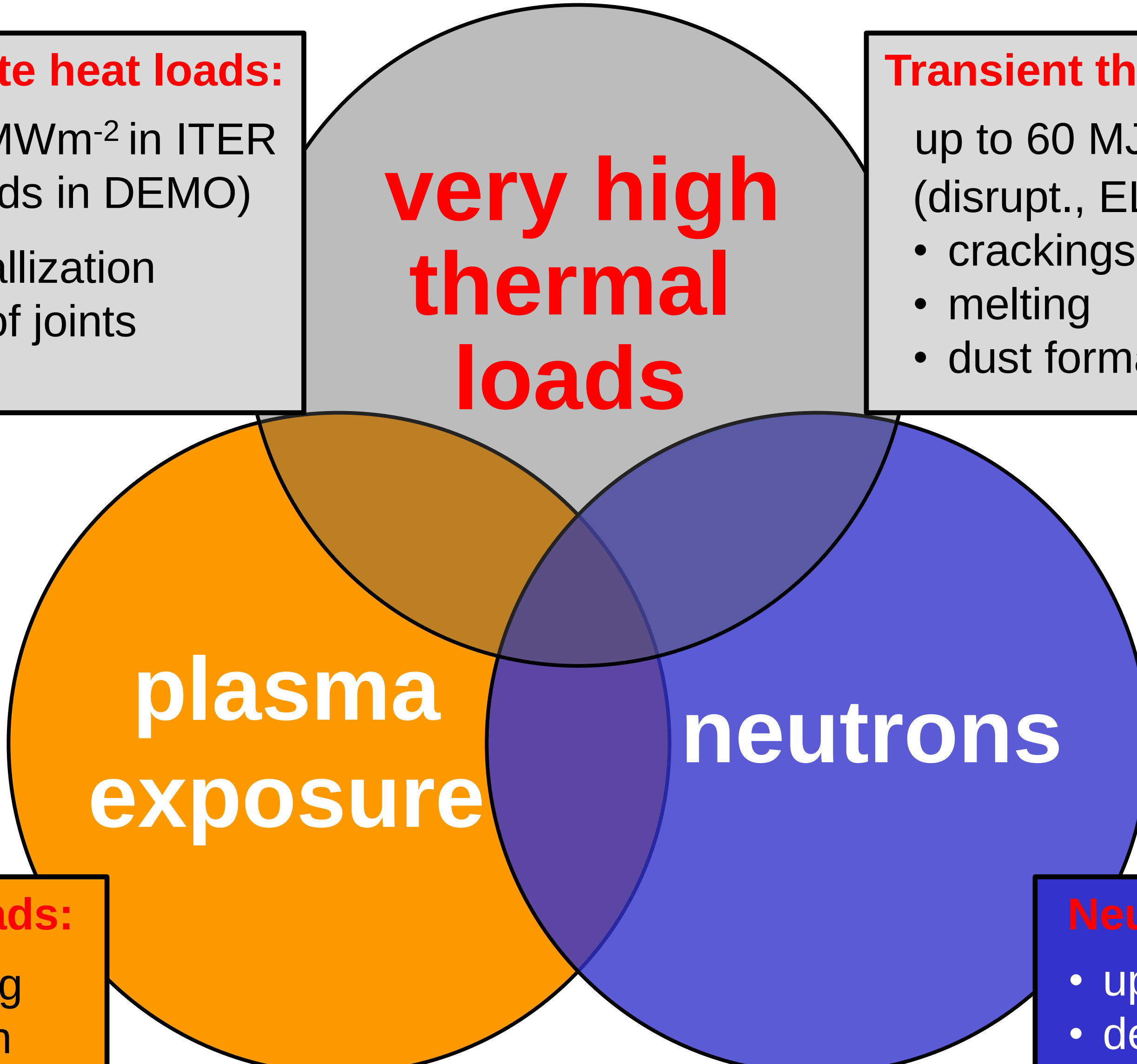

Plasma loads:

- sputtering
- hydrogen
- helium

Neutrons:

- up to 14 MeV
- defects
- transmutation

Facilities at FZJ

Electron beam facility JUDITH 1

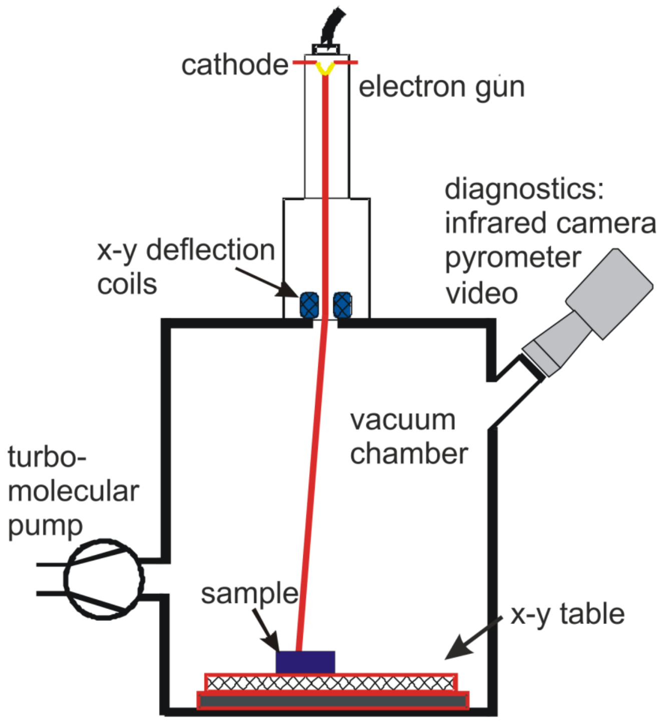

- max. power 60 kW
- acceleration voltage < 150 kV
- EB diameter ~1 mm (FWHM)

Linear plasma device PSI-2

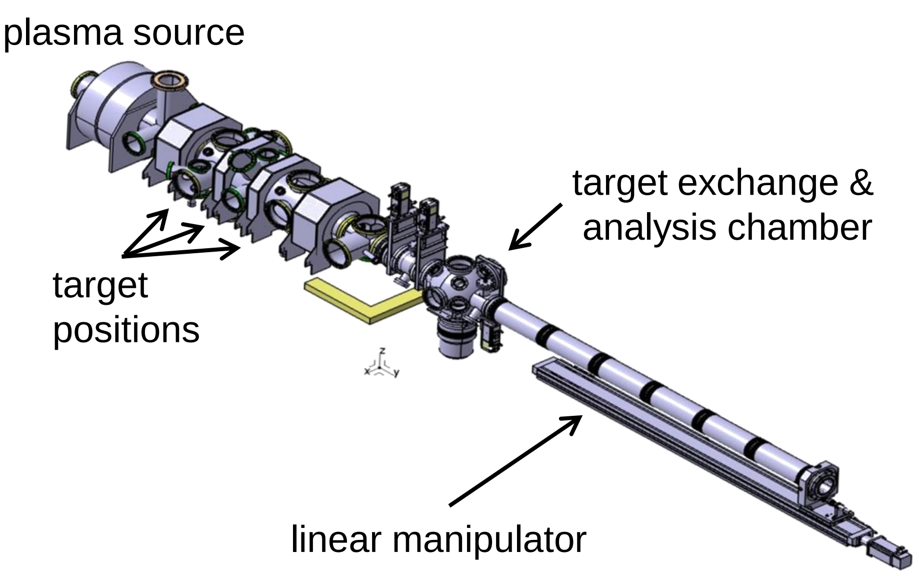

- plasma diameter 60 mm
- particle flux ≤ 10^{23} $m^{-2}s^{-1}$
- incident ion energy (bias) 10 – 300 eV
- Nd:YAG laser 1064 nm
- laser energy 32 J

B

Low and high pulse number test

Environmental conditions

Expected heat loads in ITER divertor:

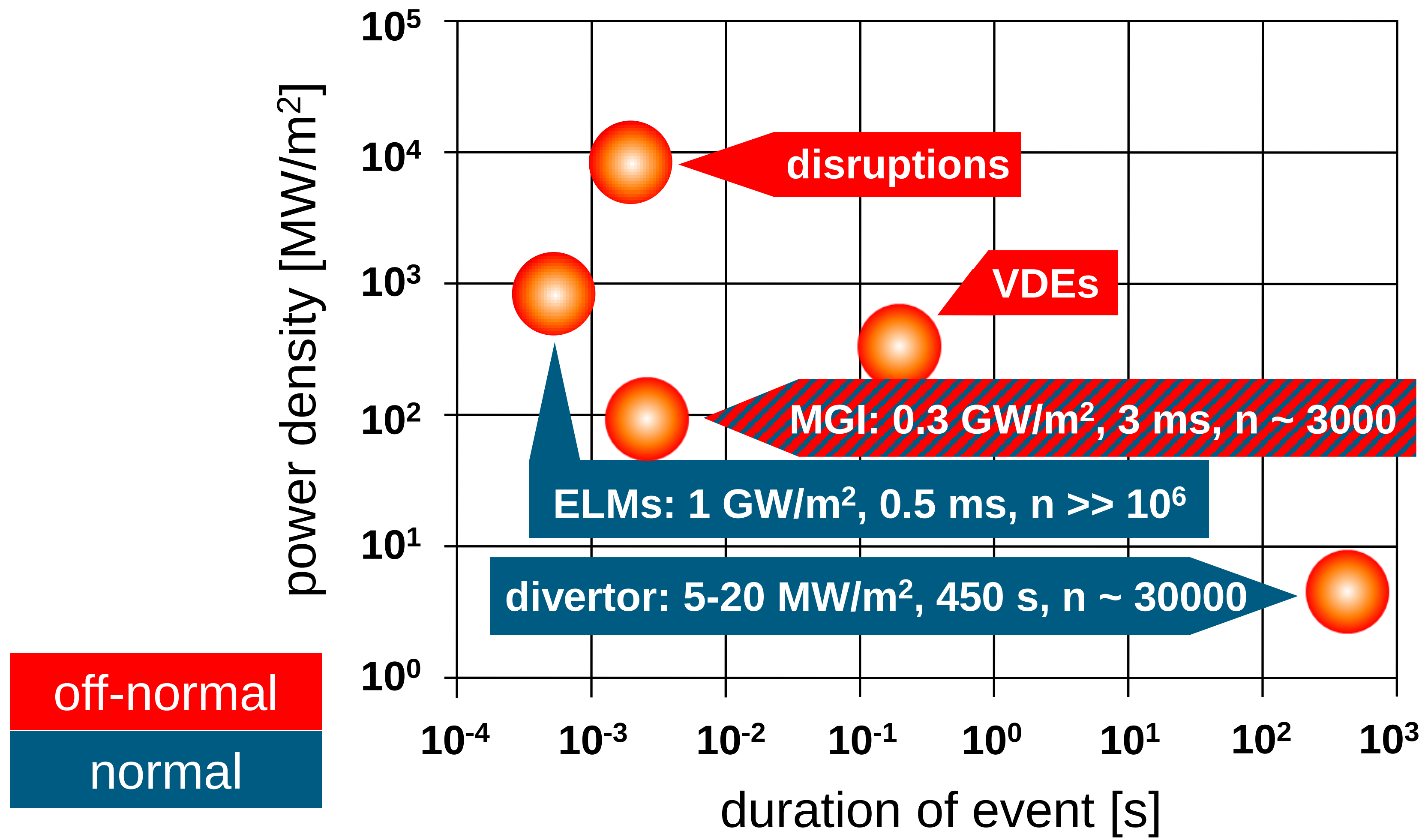

R. A. Pitts, et al., Journal of Nuclear Materials 438 (2013) S48-S56
J. Linke, Transactions of fusion science and technology 49 (2006) 455-464
A. Loarte et al., Plasma Physics and Controlled Fusion 45 (2003) 1549-1569

Mechanical properties

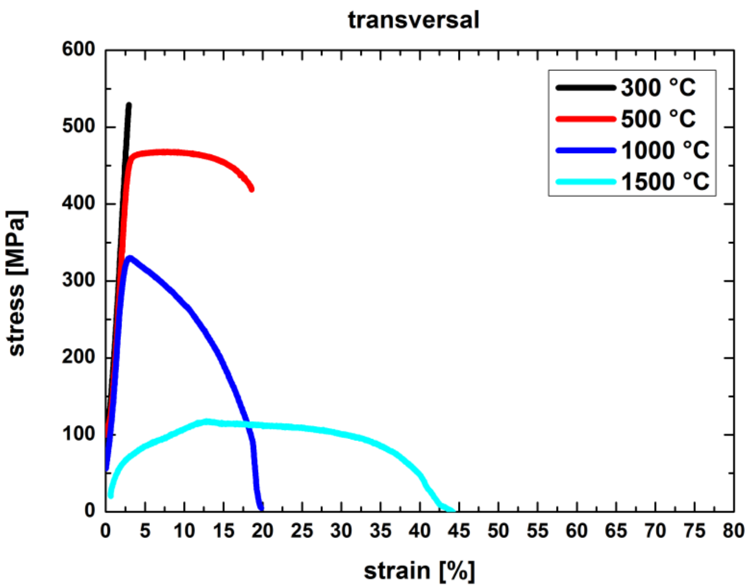

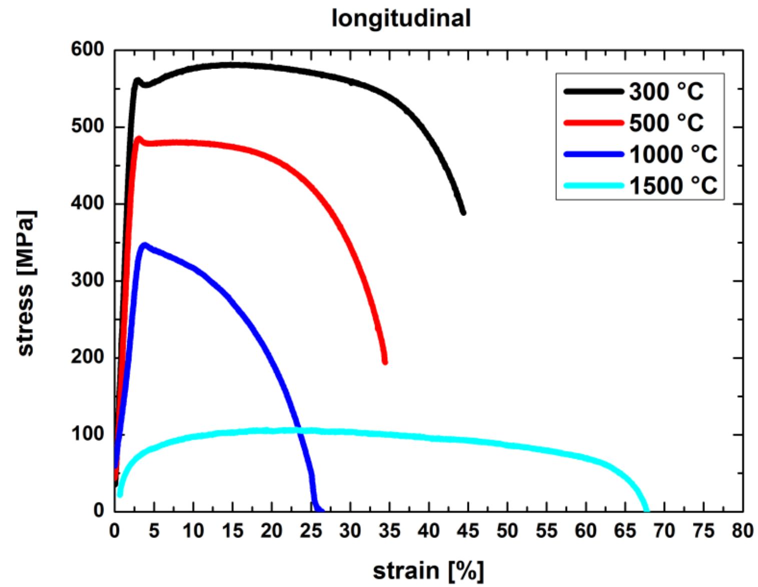

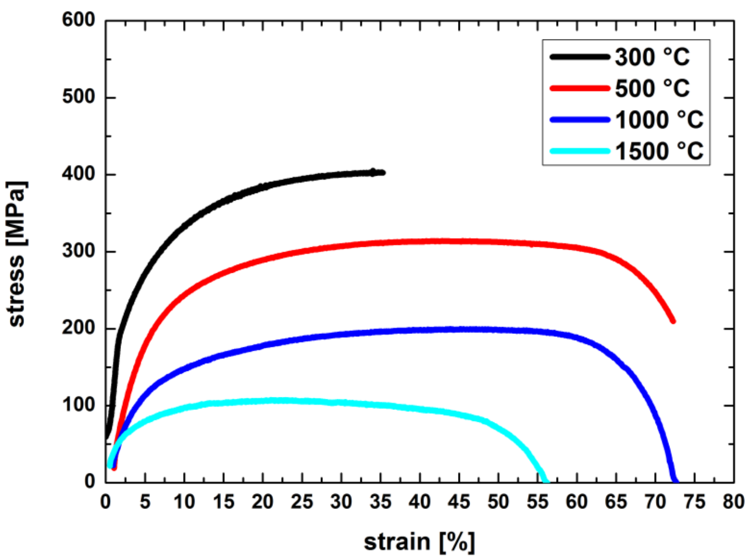

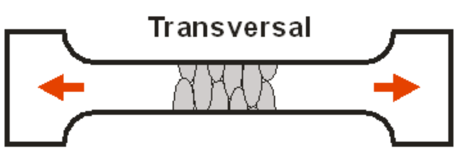

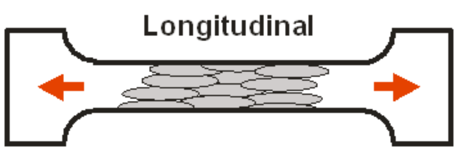

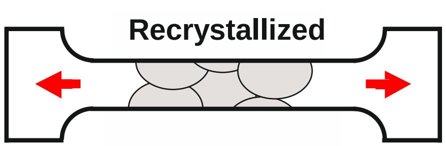

Tensile tests

deformation speed: 0.2 mm/min

deformation rate: 10^{-4} s^{-1}

Thermal shock - damage mapping

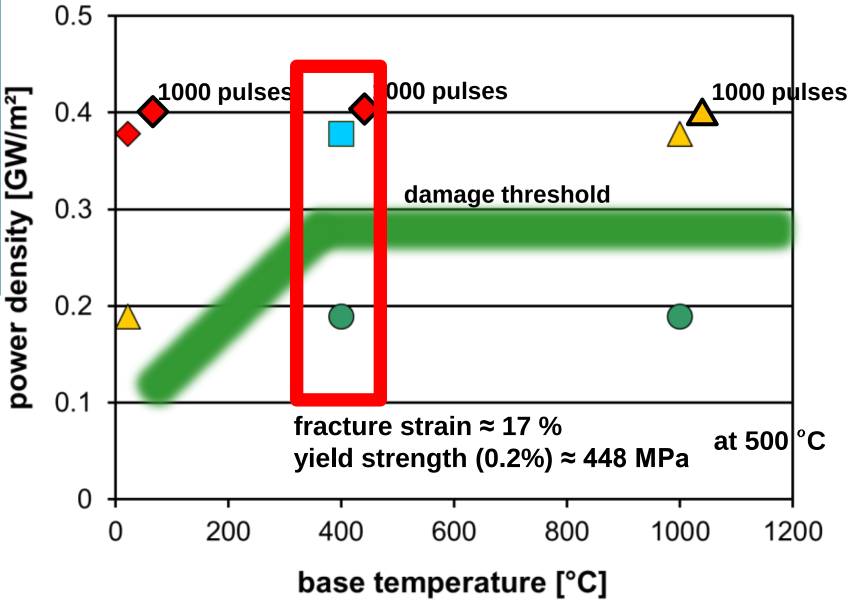

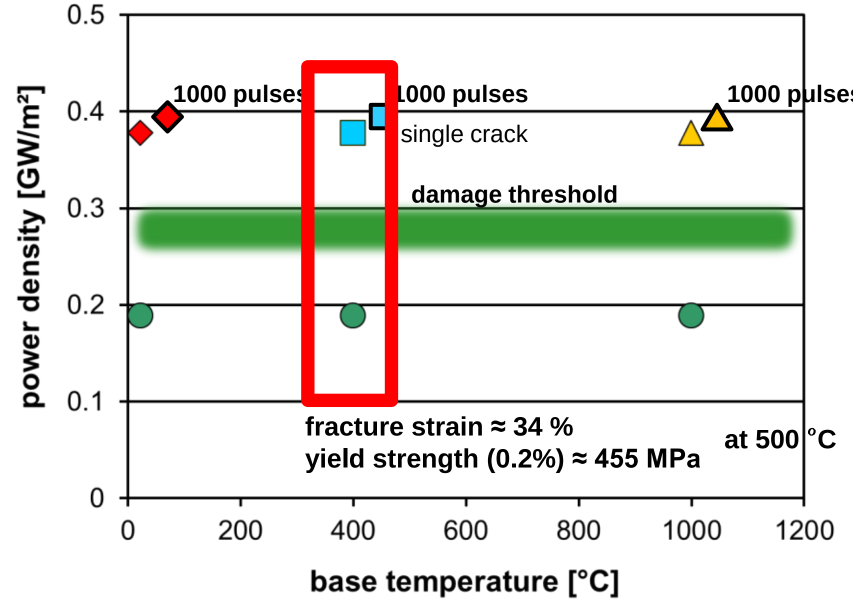

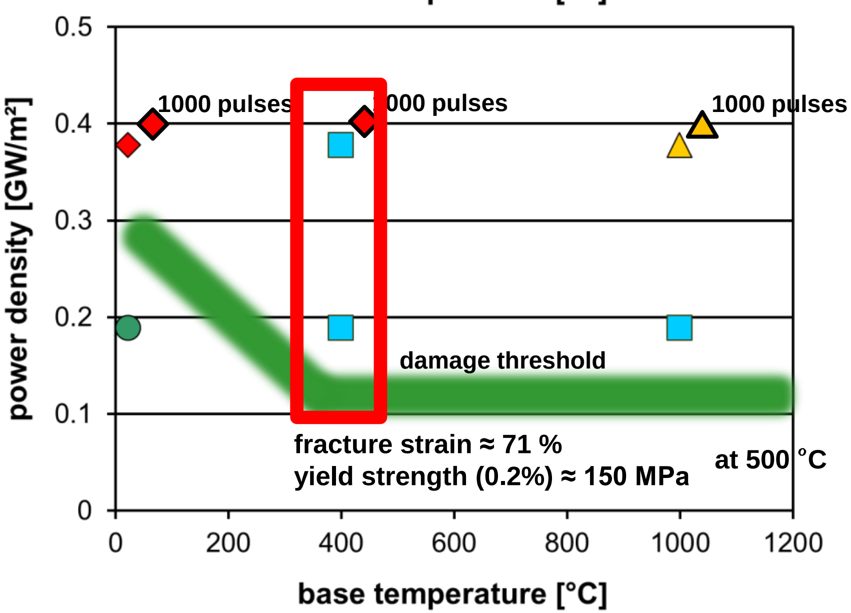

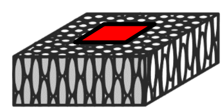

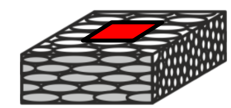

- no damage
- surface modification
- small cracks
- crack network

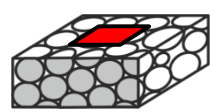

pulse duration 1 ms
100/1000 pulses

absorption coefficient: 0.55

High pulse number tests

Tungsten at high pulse numbers

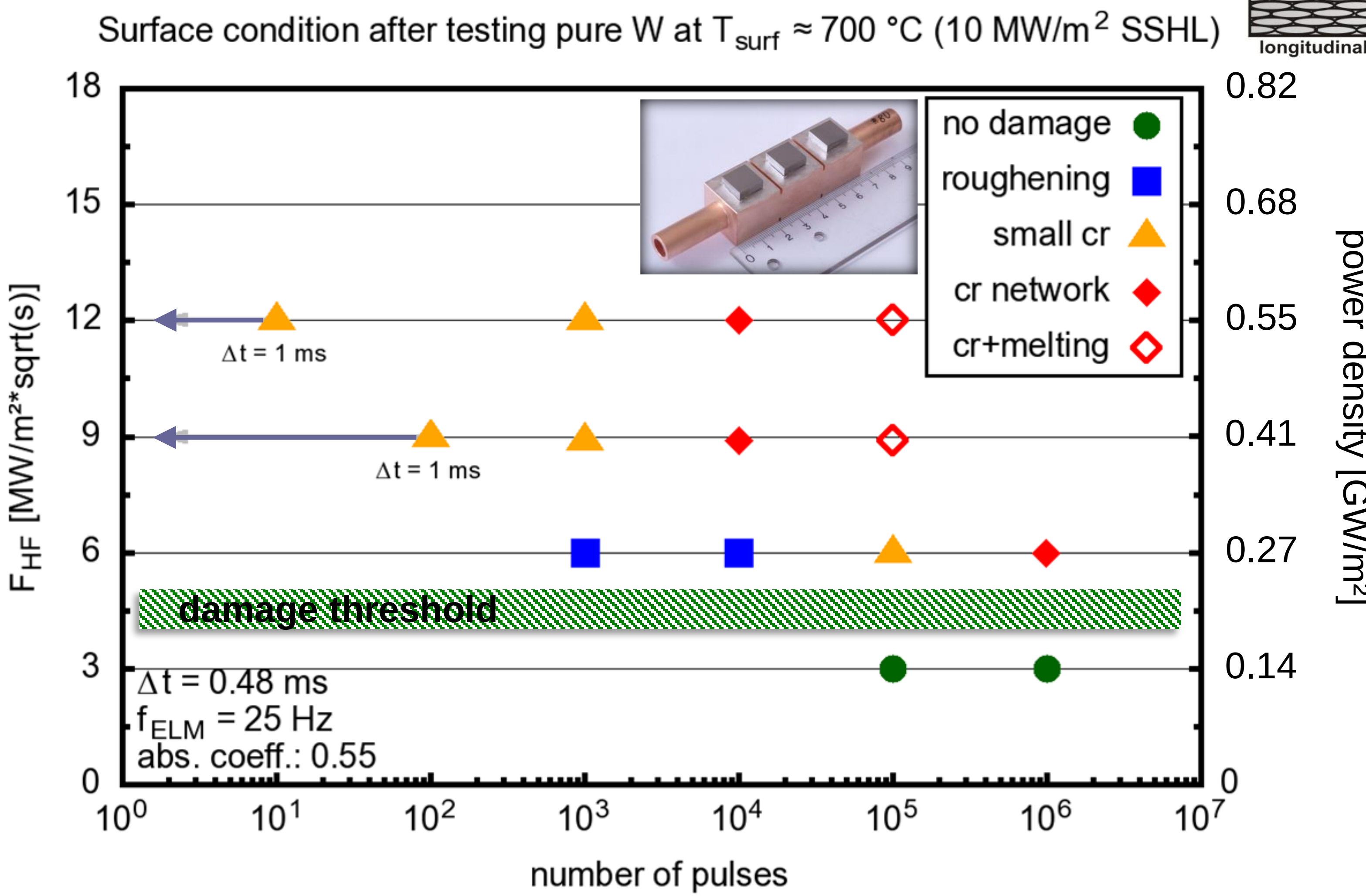

Th. Loewenhoff et al., Physica Scripta T145 (2011) 014057

High pulse number tests

Tungsten at high pulse numbers

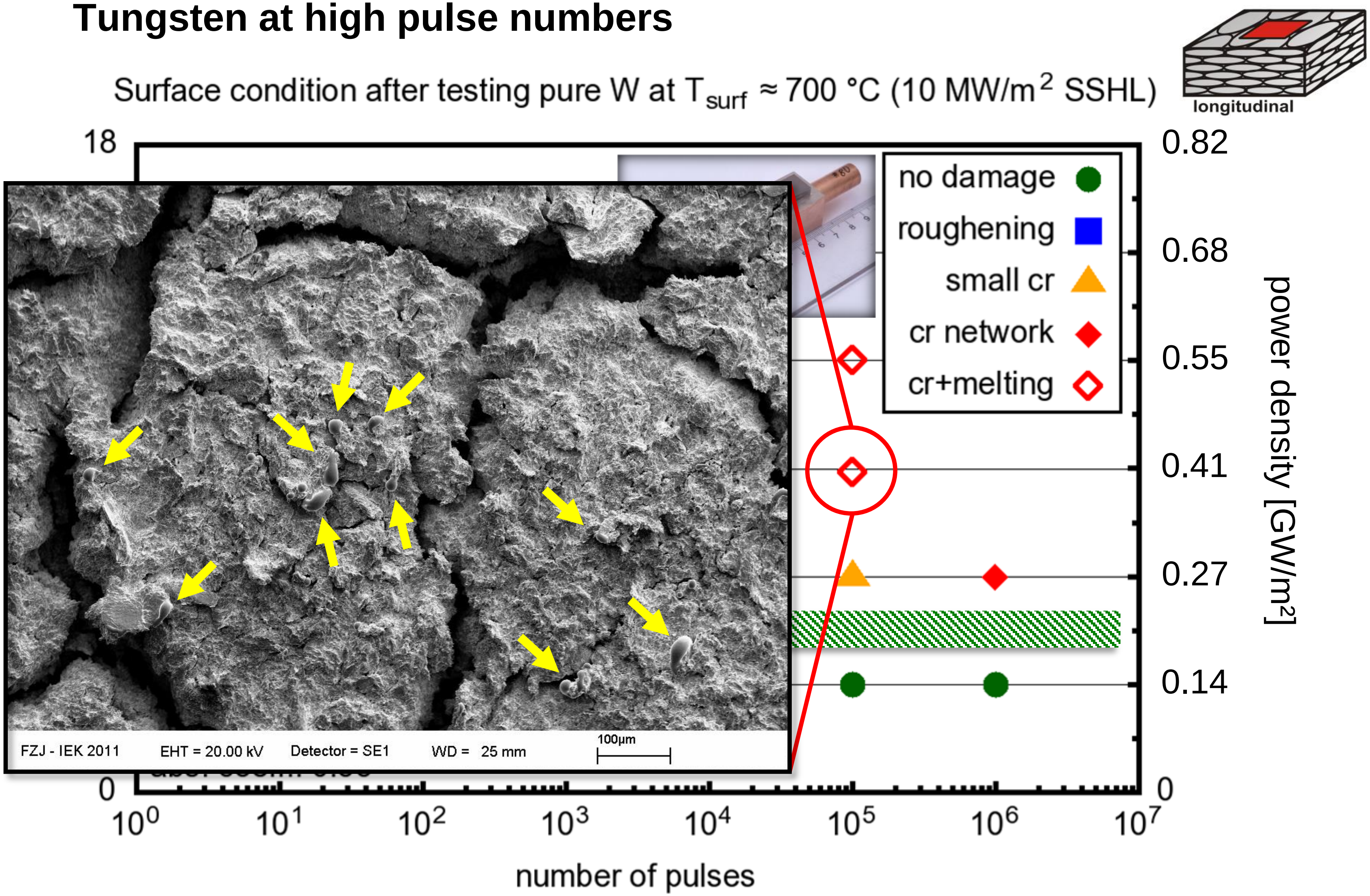

Th. Loewenhoff et al., Physica Scripta T145 (2011) 014057

Investigation of fatigue effects

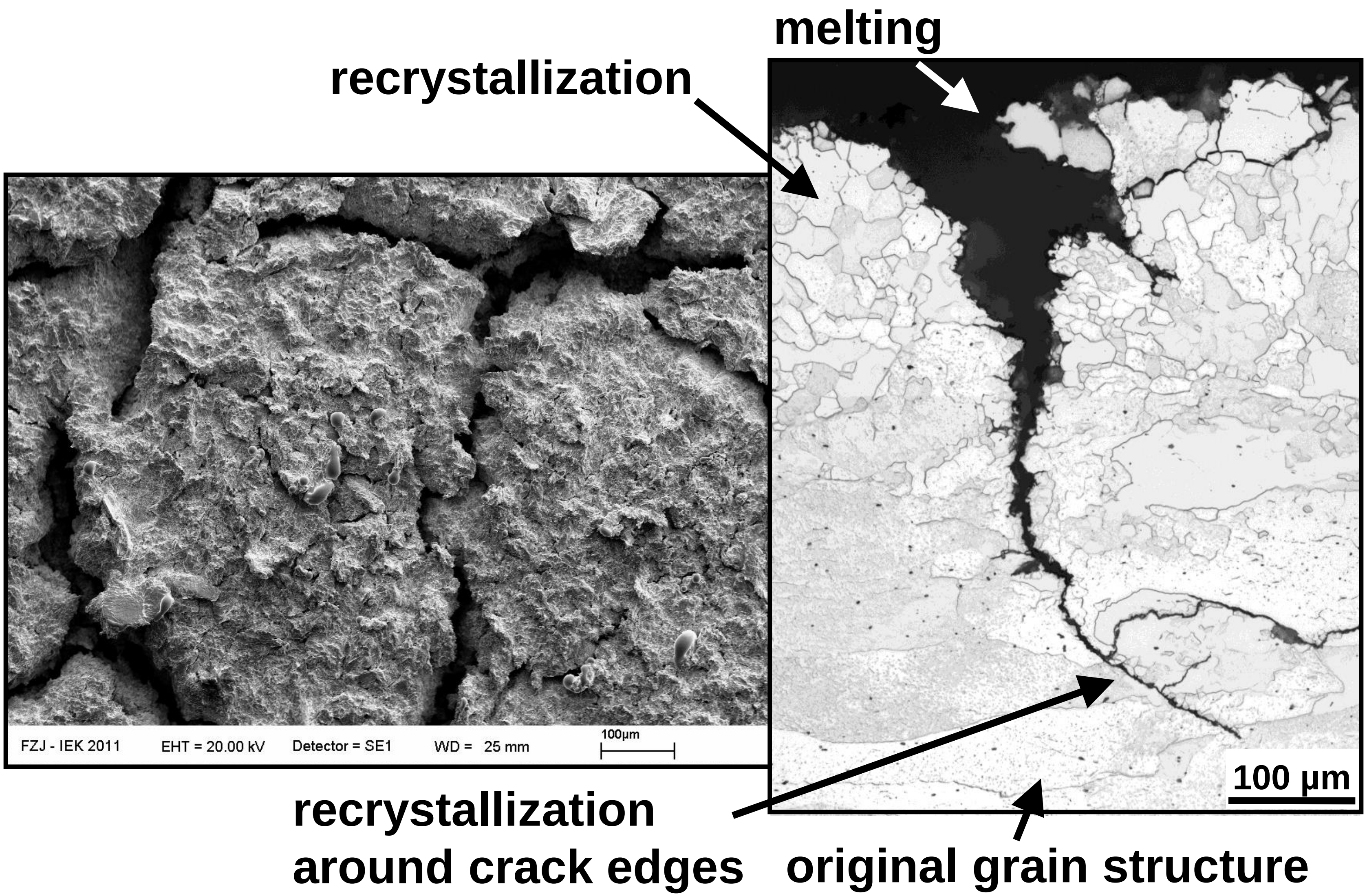

Th. Loewenhoff et al., Fusion Engineering and Design 87 (2012), 1201-1205

Influence of microstructure

Tungsten at high pulse numbers

Surface condition after testing pure W at $T_{surf} \approx 700$ °C (10 MW/m^2 SSHL)

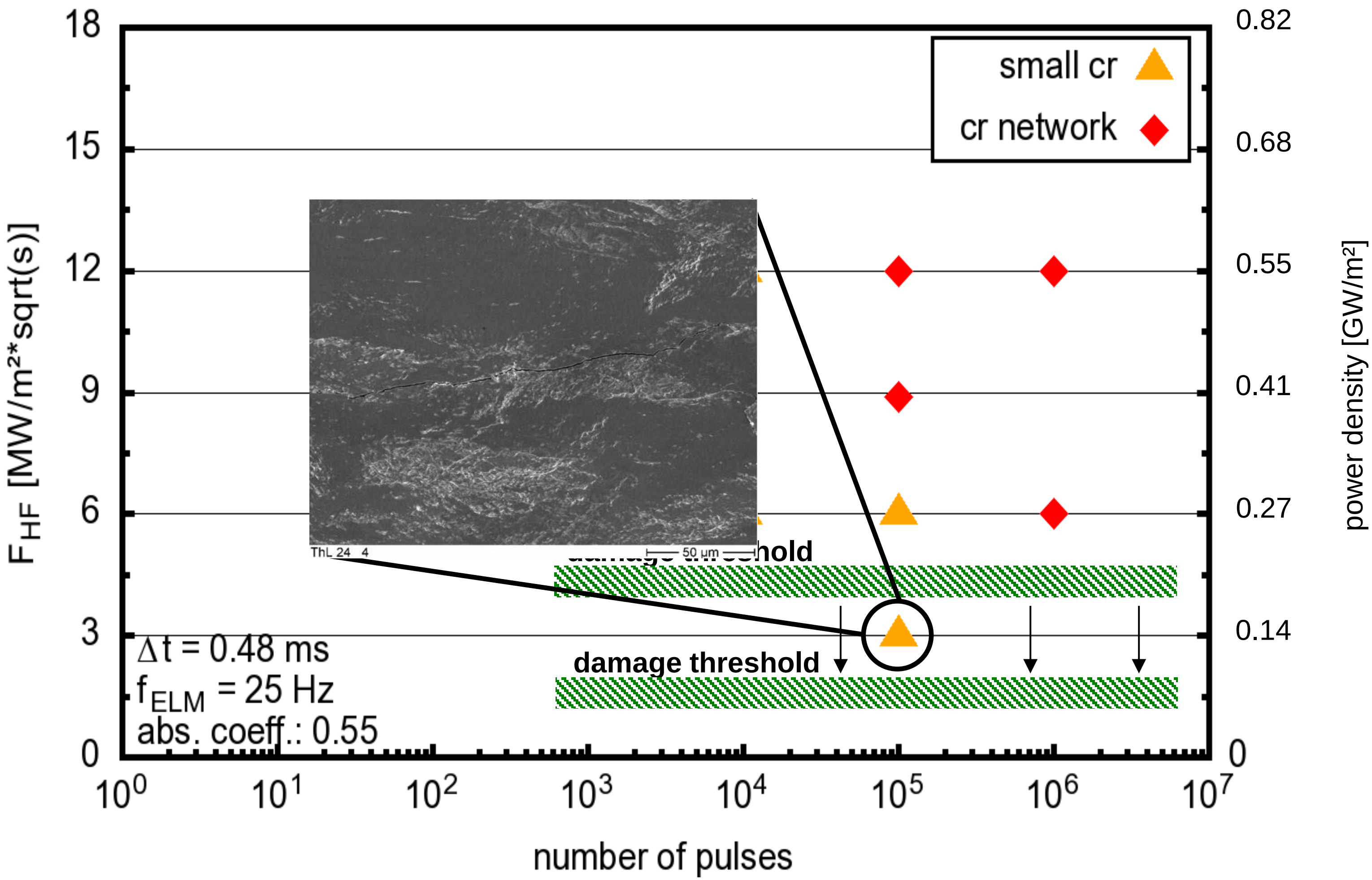

Tungsten at high pulse numbers

Surface condition after testing pure W at T_{surf} ≈ 700 °C (10 MW/m^2 SSHL)

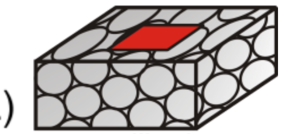

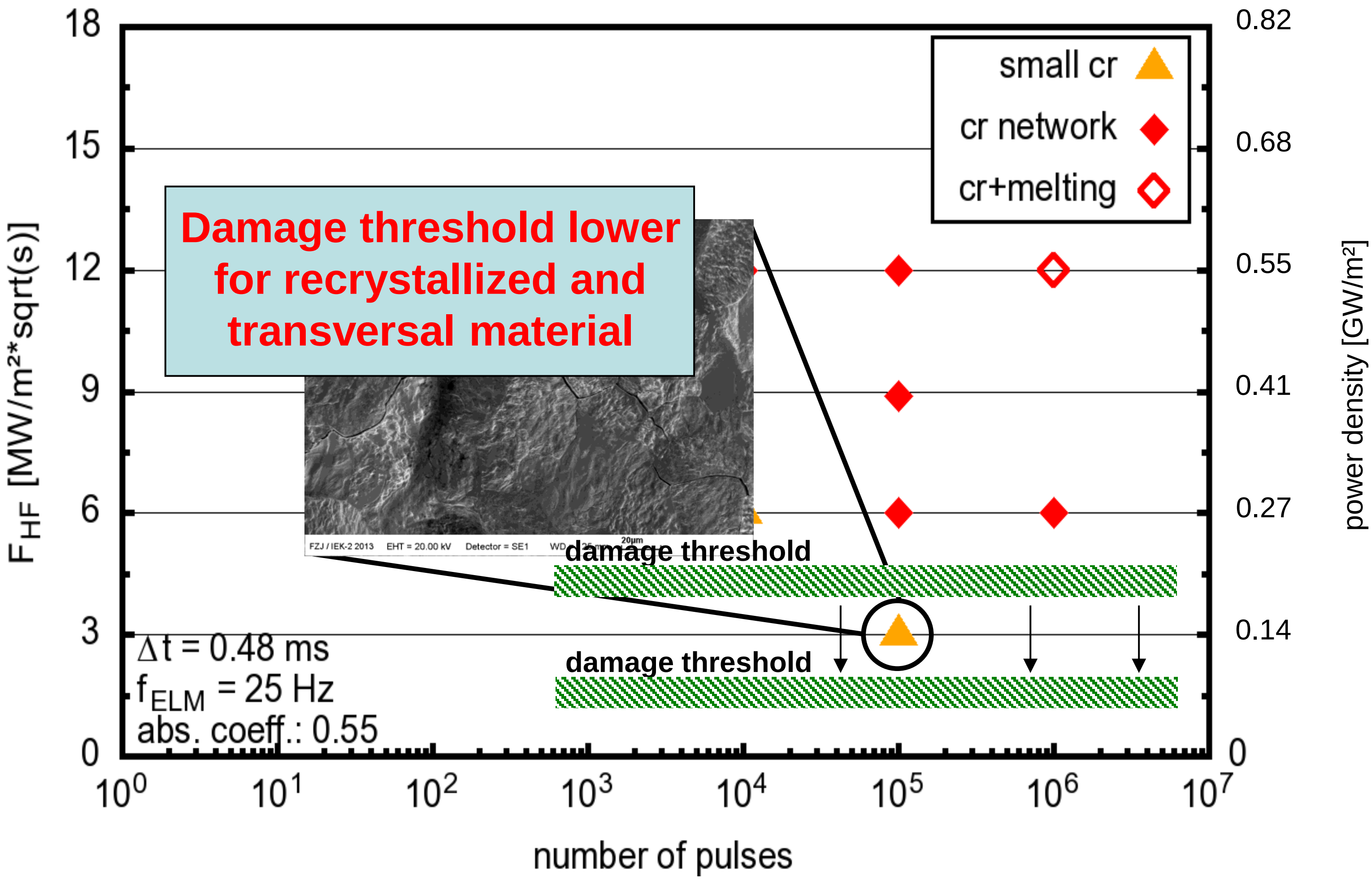

C

Combined particle and heat flux exposure of tungsten

Combined tests in PSI-2

- commercially available sintered tungsten product
- representative example:

Transversal

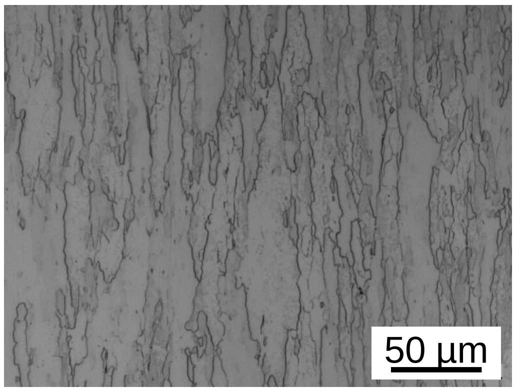

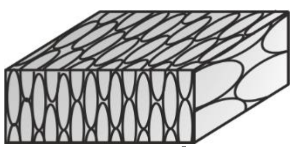

transversal

at 1000 °C
fracture strain ≈ 22 %
yield strength (0.2%) ≈ 370 MPa

Longitudinal

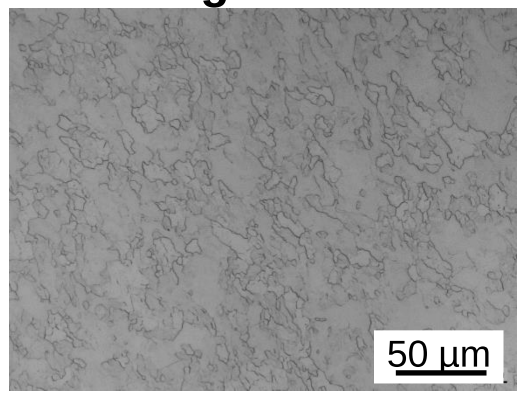

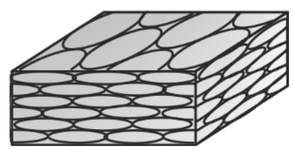

longitudinal

at 1000 °C
fracture strain ≈ 17 %
yield strength (0.2%) ≈ 340 MPa

Recrystallized

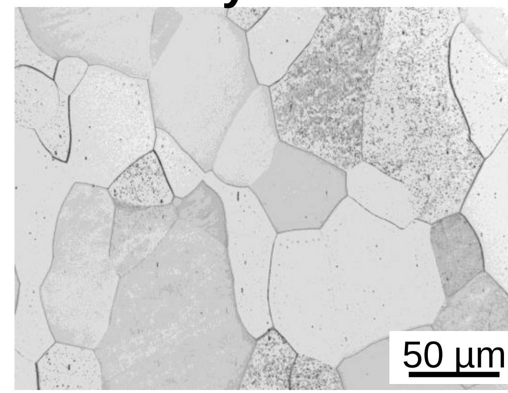

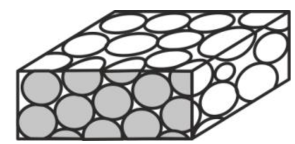

recrystallized **1600 °C, 1 h**

at 1000 °C
fracture strain ≈ 68 %
yield strength (0.2%) ≈ 100 MPa

- characterization of the high pulse number thermal shock performance (fatigue) with steady state particle background

High pulse number tests in PSI-2

Laser beam

ELM-like heat loads at 730 °C
absorbed power density: 0.38 GW/m²
pulse duration: 0.5 ms (f = 10 Hz)

H/He (6 %) - Plasma

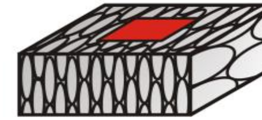

particle energy ≈ 35 eV
plasma flux ≈ $6.0 \times 10^{21}\ m^{-2}s^{-1}$
fluence ≈ $9.0 \times 10^{24}\ m^{-2}$ / $6.0 \times 10^{25}\ m^{-2}$

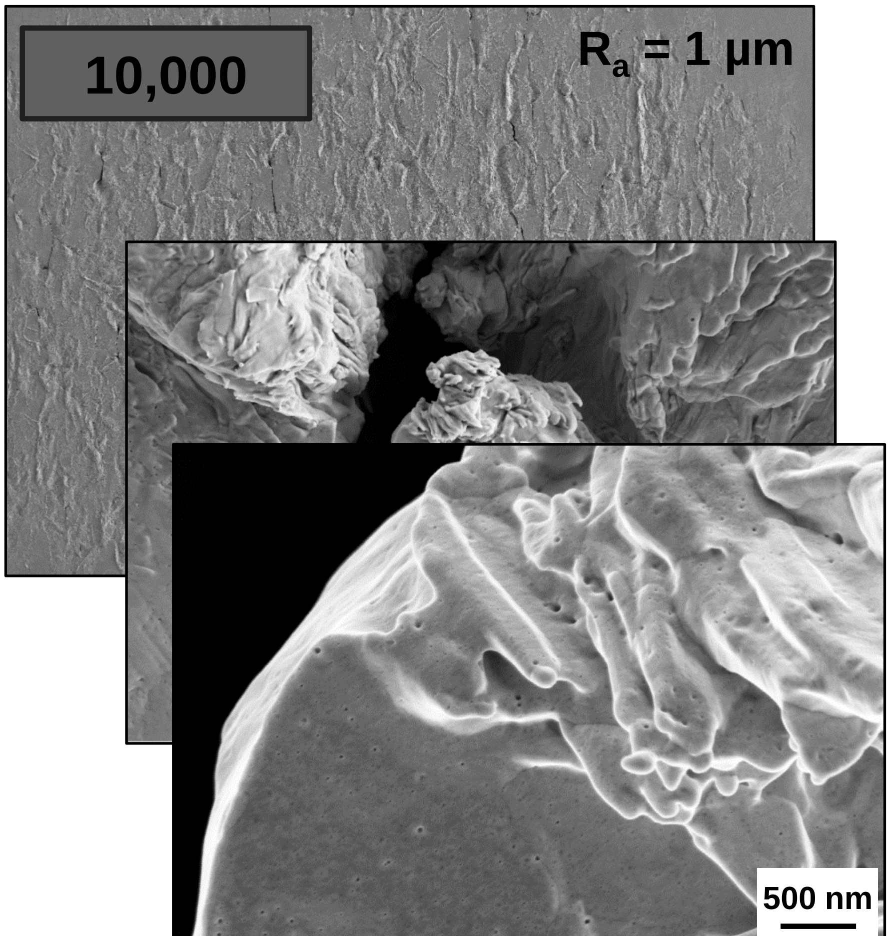

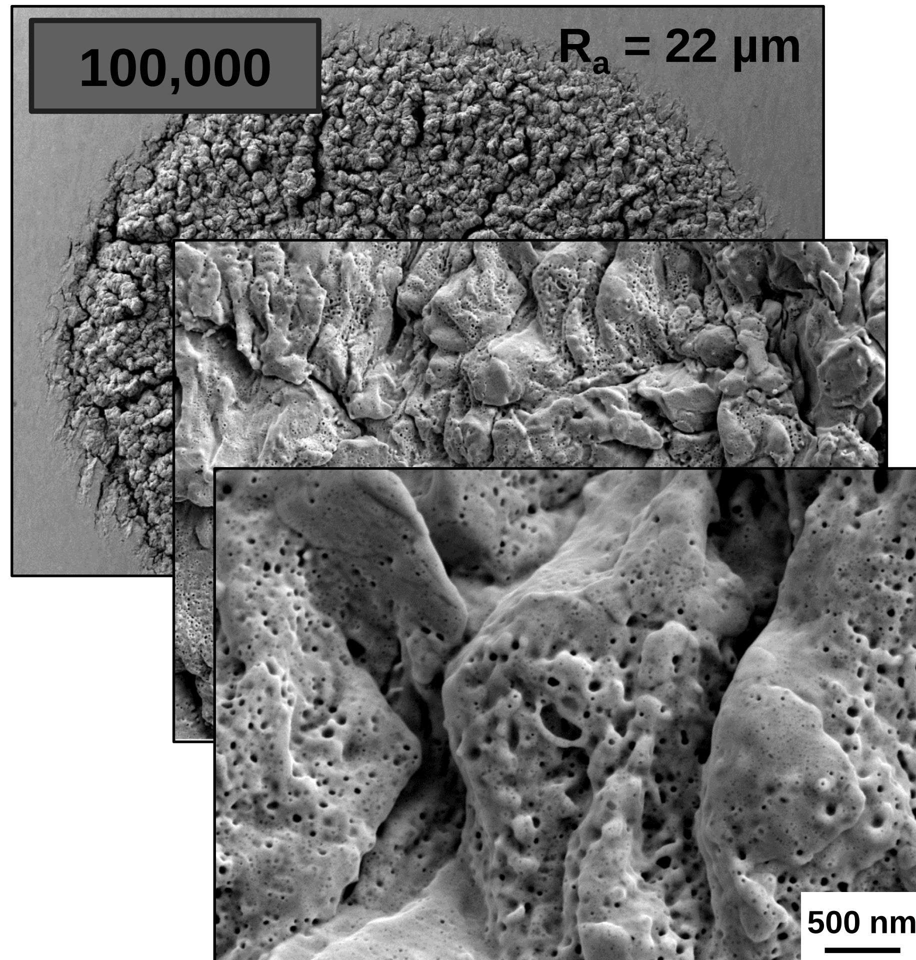

High pulse number tests in PSI-2

10,000 pulses

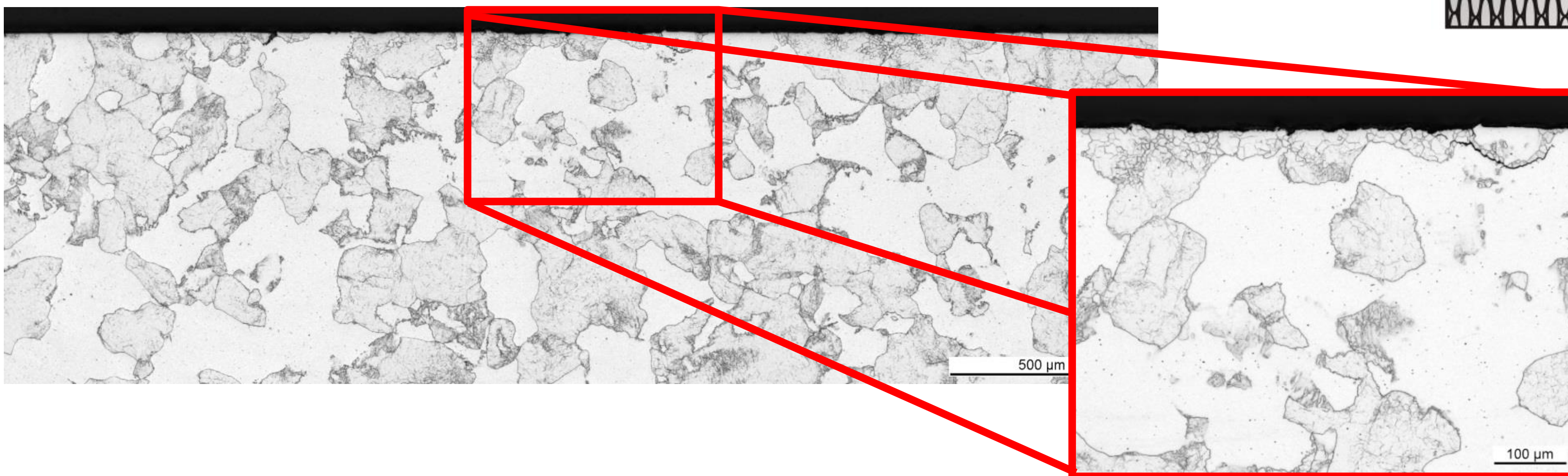

100,000 pulses

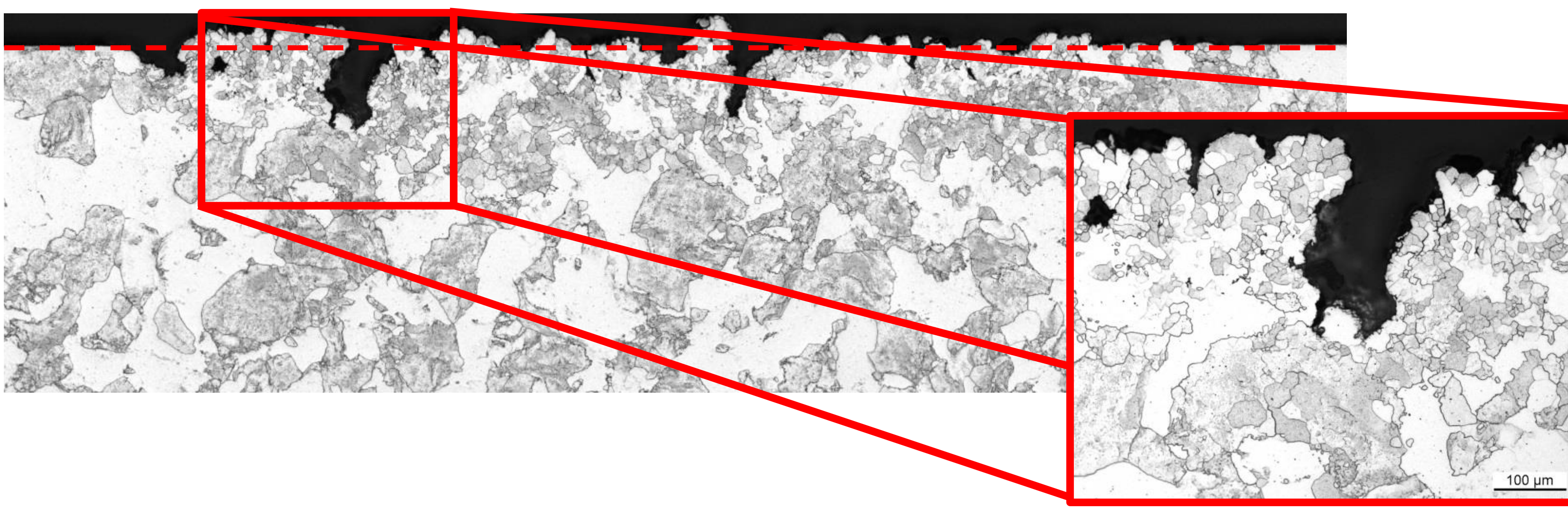

Surface roughness and structure

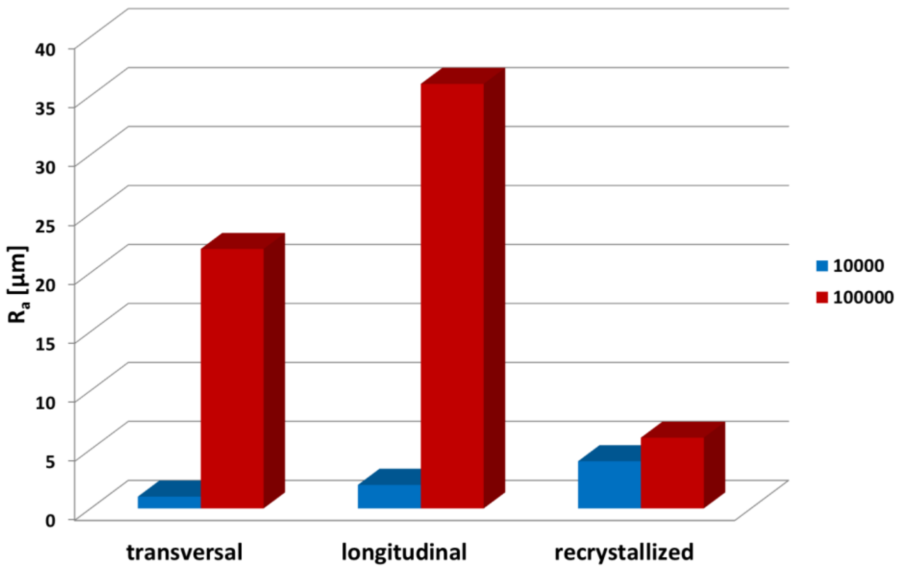

Arithmetic mean roughness (R_a)

- significant increase for higher number of pulses (accumulation of plastic deformation)
- high strength/low ductility of the transversal and longitudinal grain orientation leads to severe damage
- lower strength/higher ductility of the recrystallized materials leads to a faster damage evolution but lower R_a values after high pulse numbers

Hill and valley structure after 100,000 pulses

- severe hill and valley structure
- height differences up to 425 µm
- could be an indication for erosion of large parts of the surface (dust formation, plasma contamination)
- enhanced risk of overheating/melting, especially for low angle of incident

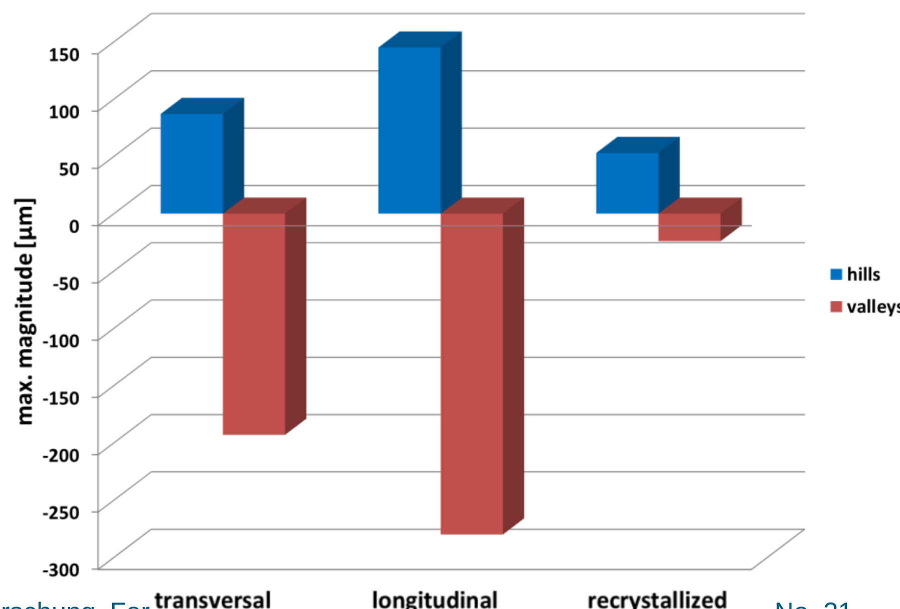

Comparison PSI-2 and JUDITH 2

100,000 pulses

PSI-2 (laser + plasma)

JUDITH 2 (pure thermal)

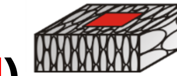

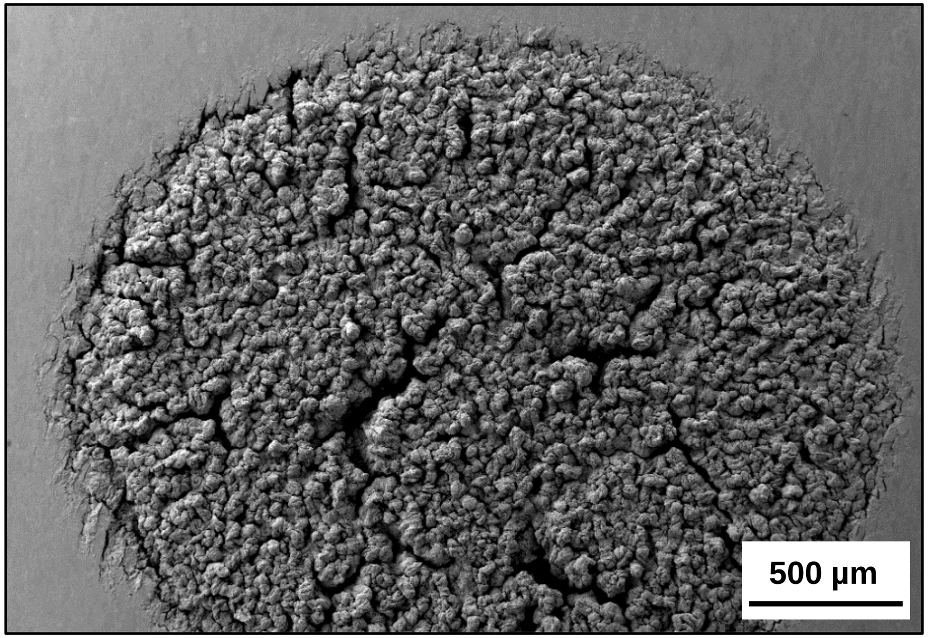

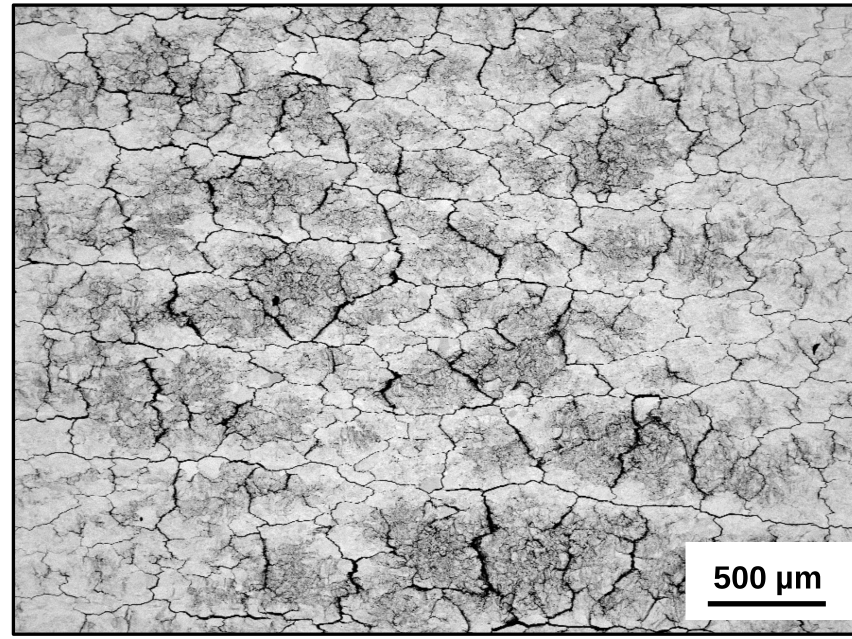

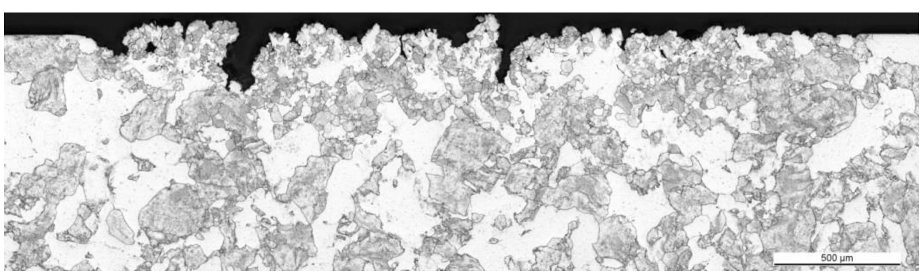

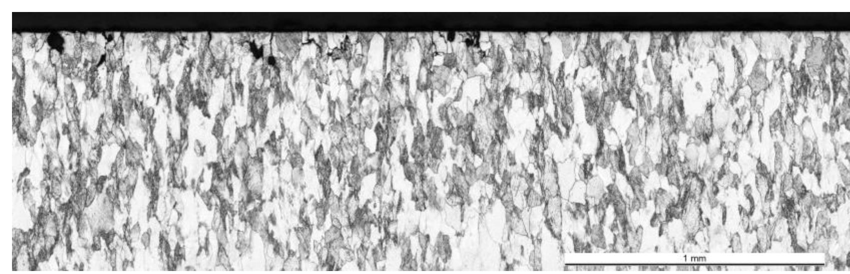

Surface modifications

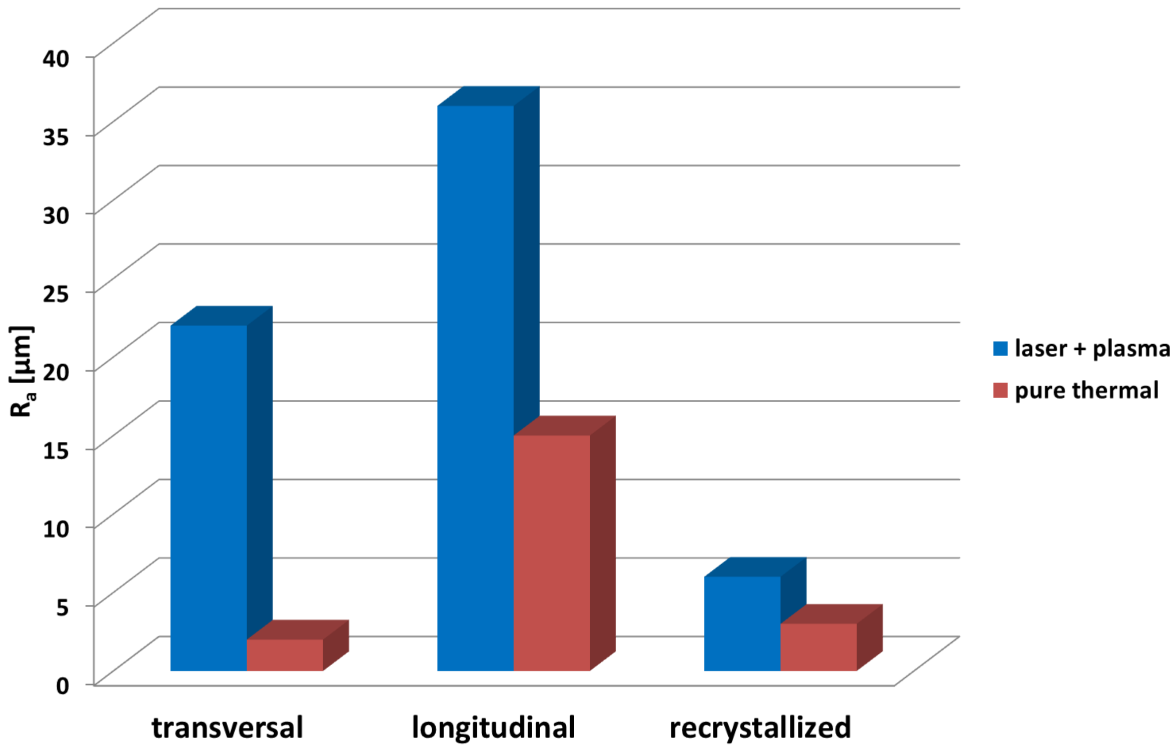

Comparison PSI-2 (laser + plasma) and JUDITH 2 (pure thermal)

- combination of steady state particle background with transient thermal loads leads to a much faster damage evolution (fatigue) compared to pure thermal (⇒ H/He embrittlement, degradation of mechanical strength)
- effect of lower strength/higher ductility of the recrystallized materials also reflected in the pure thermal results

Th. Loewenhoff et al., Fusion Engineering and Design 87 (2012), 1201-1205

Microstructural changes

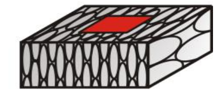

10,000 pulses **100,000 pulses**

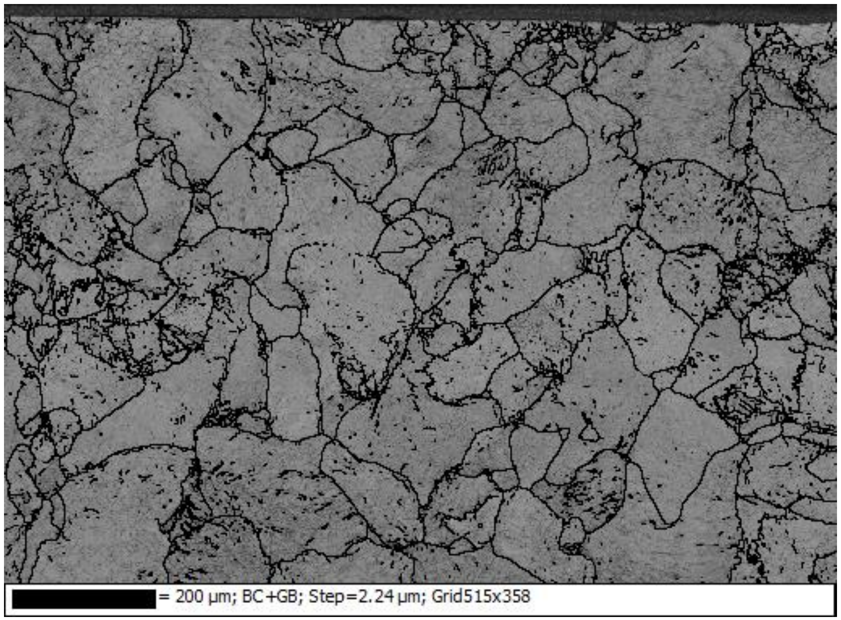

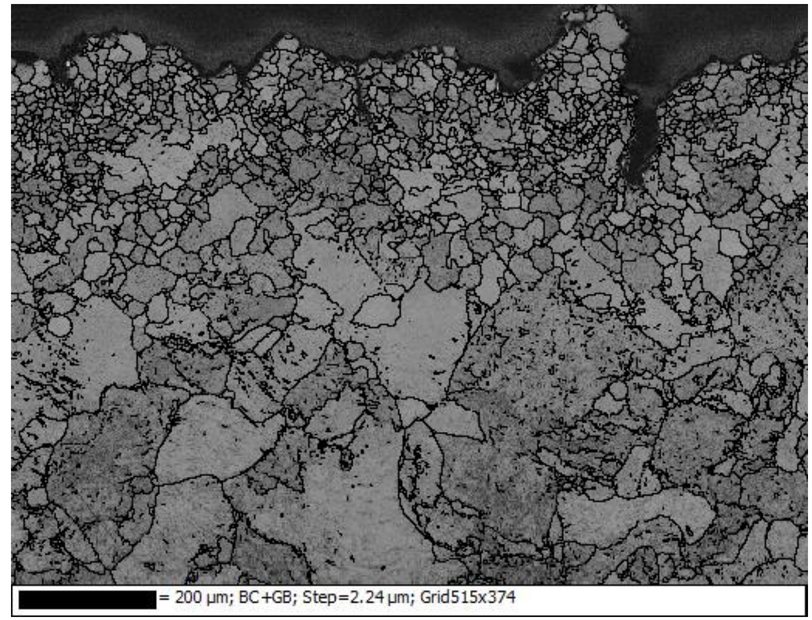

EBSD Band Contrast Image + Grain Boundaries (≥ 5°)

- near surface microstructural changes occur already after 10,000 pulses
- region increases for higher pulse numbers
- sub-grains/grain nucleation can be observed

Microstructural changes

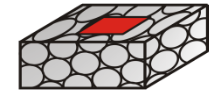

10,000 pulses

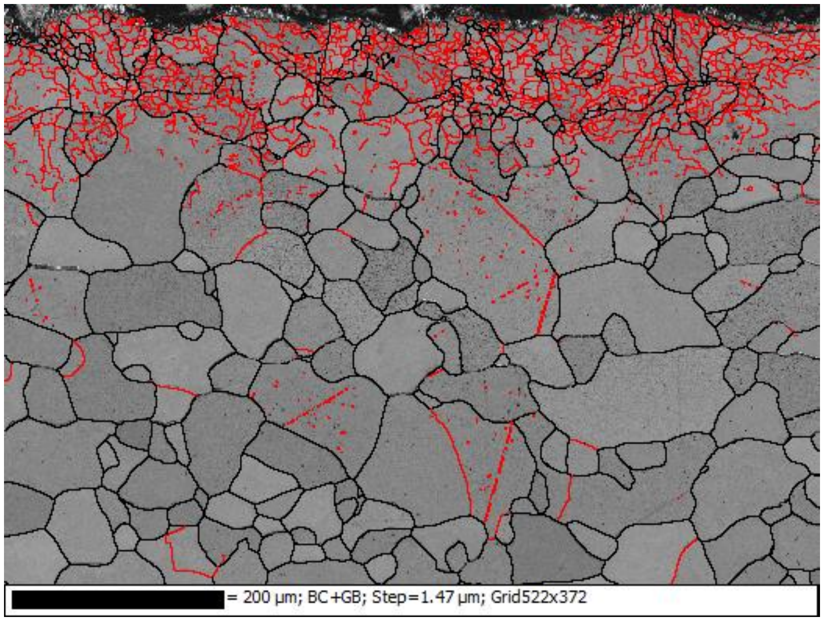

100,000 pulses

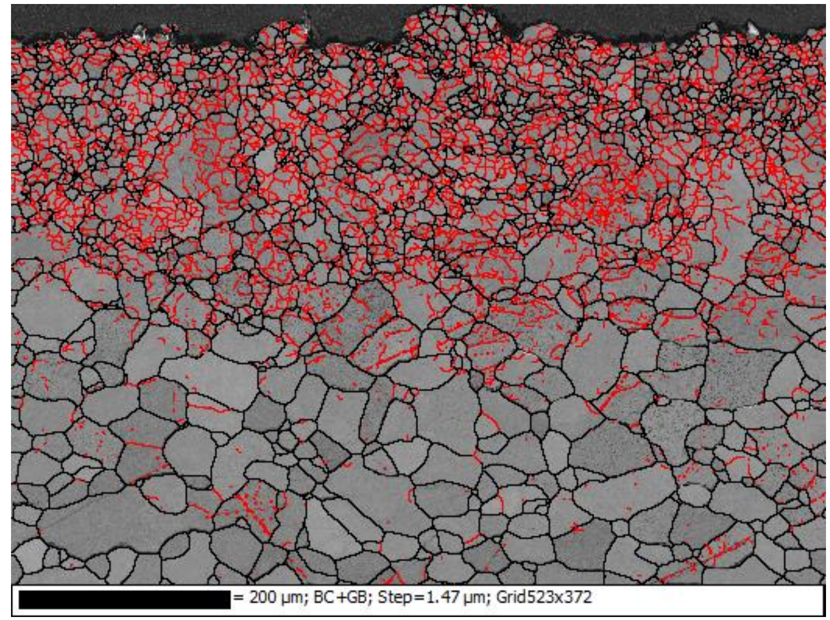

EBSD Band Contrast Image + Grain Boundaries (red: 3.5° up to 10°, black: > 10°)

- microstructural changes also visible for recrystallized material (1600 °C, 1 h)
- formation of small angle grain boundaries, grain refinement, dynamic recrystallization
- increase of the effected zone with higher number of pulses

Microstructural changes

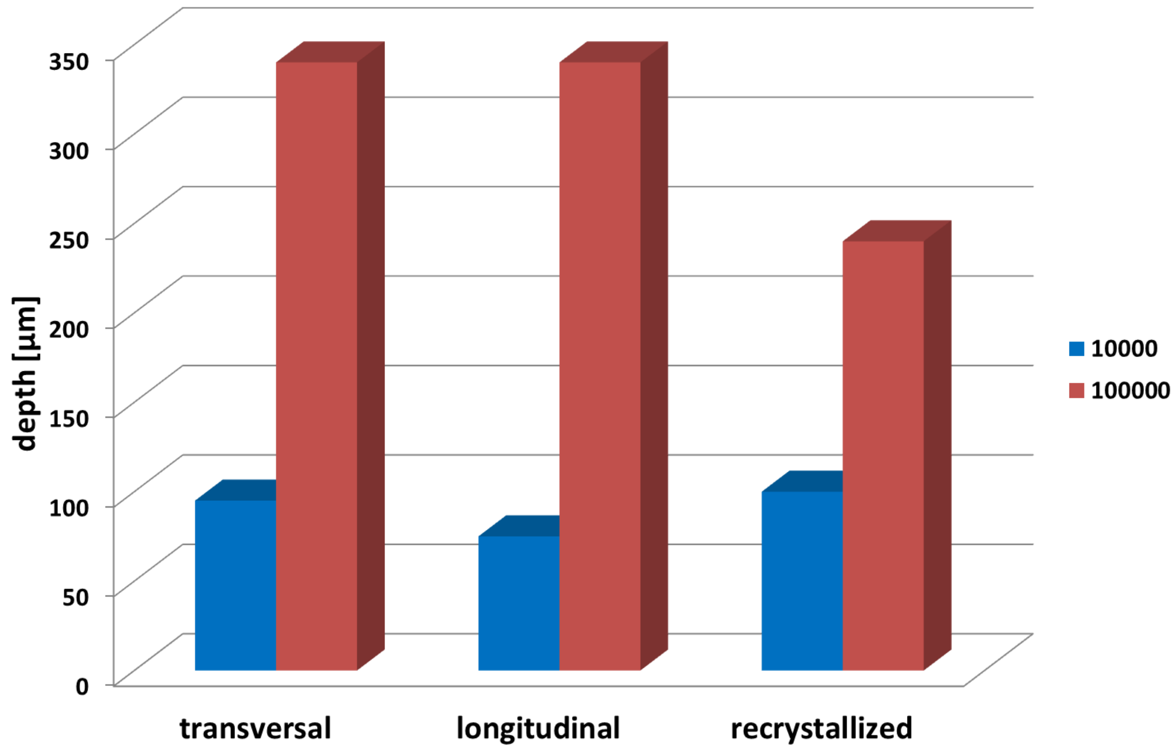

- significant increase of the depth from 10,000 to 100,000 pulses
- depth of the zone depends on the time (number of pulses) and temperature gradient ⇒ saturation for higher number of pulses?
- change of the mechanical properties in a near surface region ⇒ reduced strength/higher ductility like for the recrystallized material?
- impact on the diffusion/retention of H/He not clear ⇒ possibly higher retention as reported in: A. Huber et al. Physica Scripta T167, art. no. 014046 (2016)

Microstructural changes

100,000 pulses

PSI-2 (laser + plasma) JUDITH 2 (pure thermal)

transversal

recrystallized

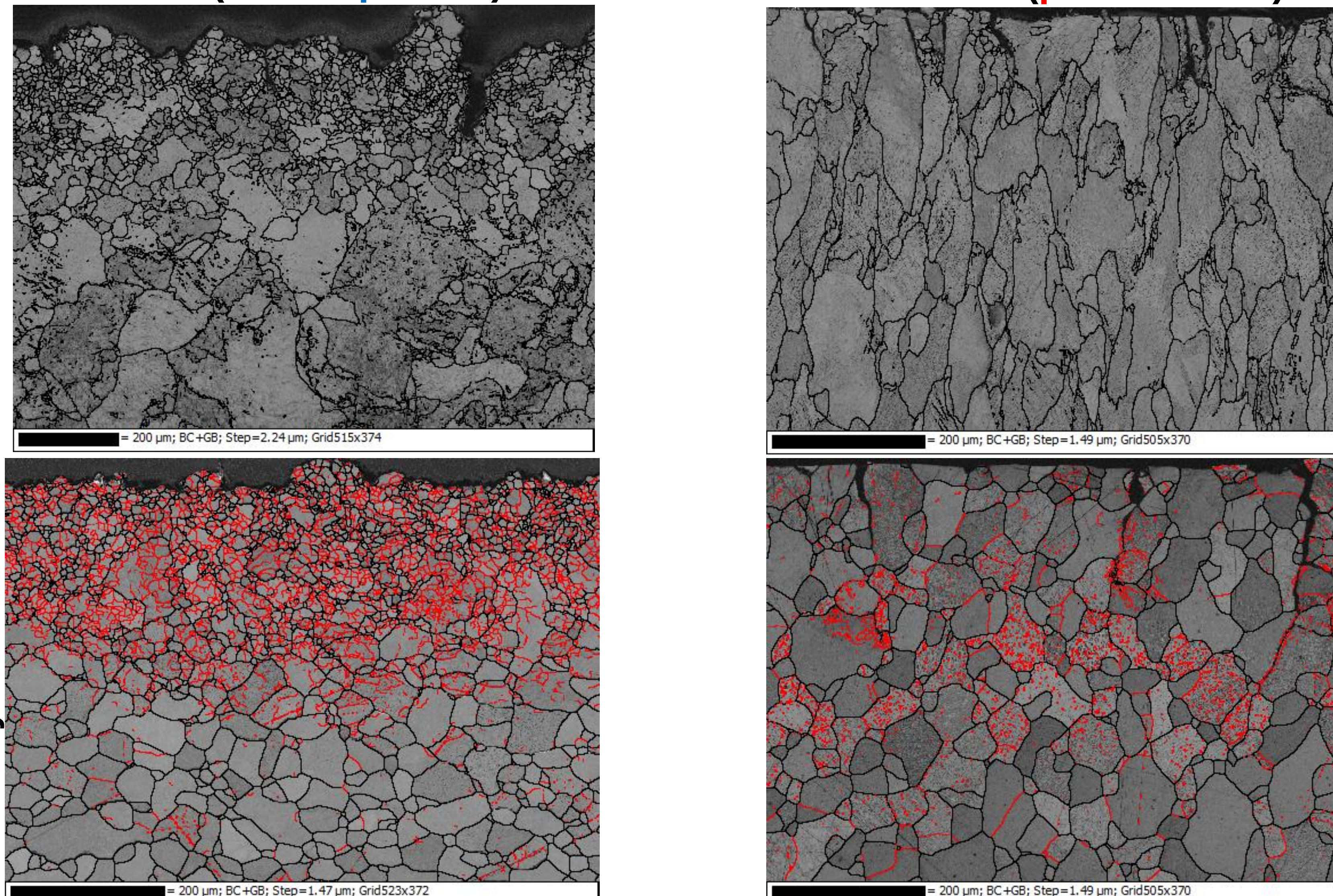

FIB cuts and He bubbles/layer

10,000 pulses

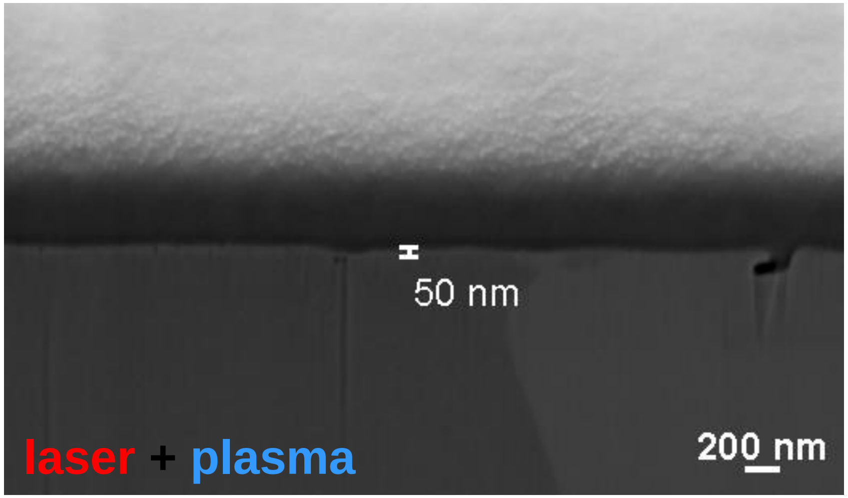

- He bubbles/layer only visible (in SEM) in the laser + plasma exposed area after 10,000 pulses
- He bubbles/layer become visible (in SEM) in the laser + plasma and only plasma exposed area after 100,000 pulses

100,000 pulses

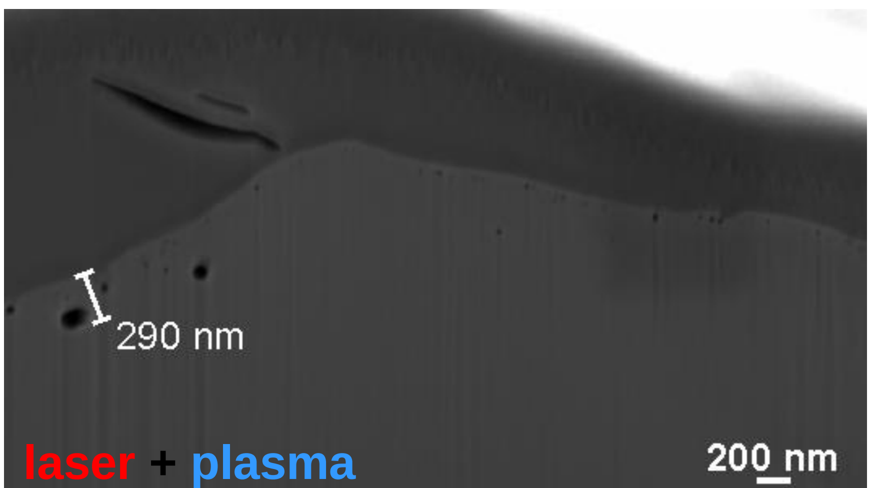

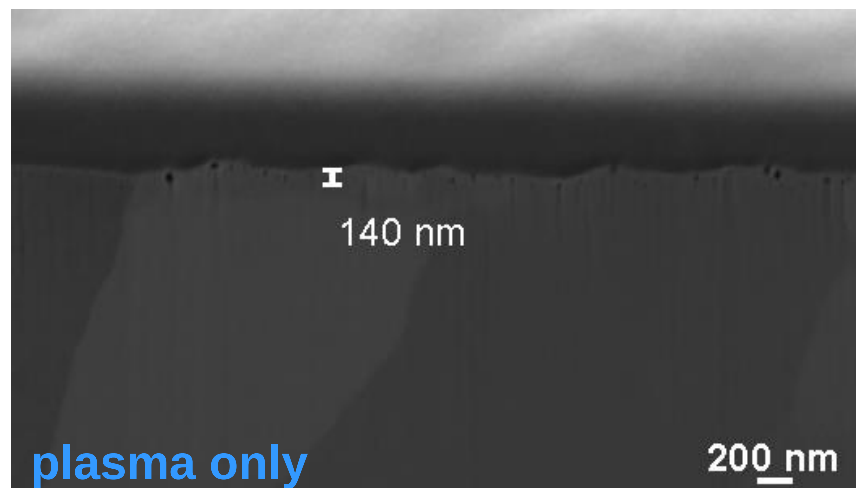

FIB cuts and He bubbles/layer

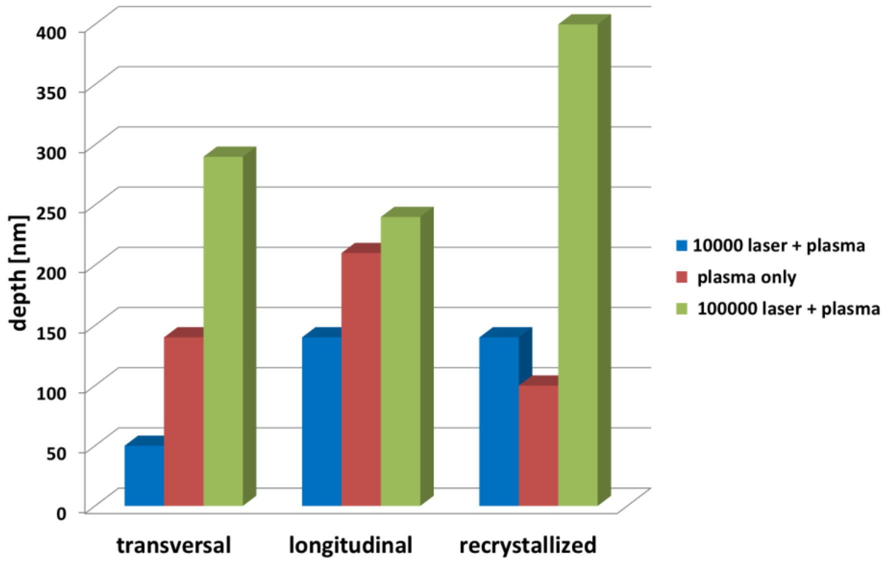

Size of the He effected layer

- depth of the He affected layer increases with number of pulses/fluence
- additional transient heat loads result in an extension of the He affected layer
- higher thermal gradients could lead to a deeper diffusion into the bulk material

Size of the visible He bubbles

- size of the visible bubbles increases for higher number of pulses/fluence
- additional transient heat loads accelerate this effect
- impact on the He bubble density not clear

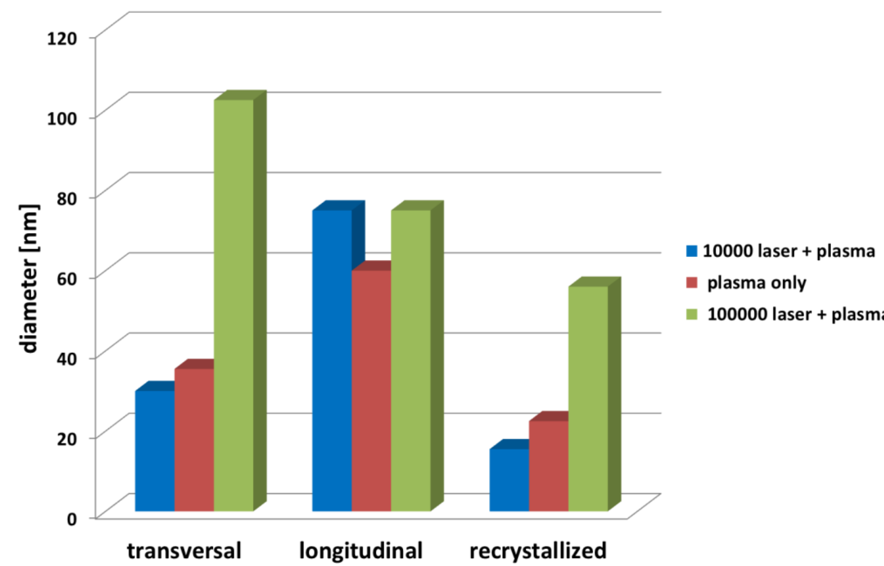

D

Tungsten characterization

W monoblock after HHF testing

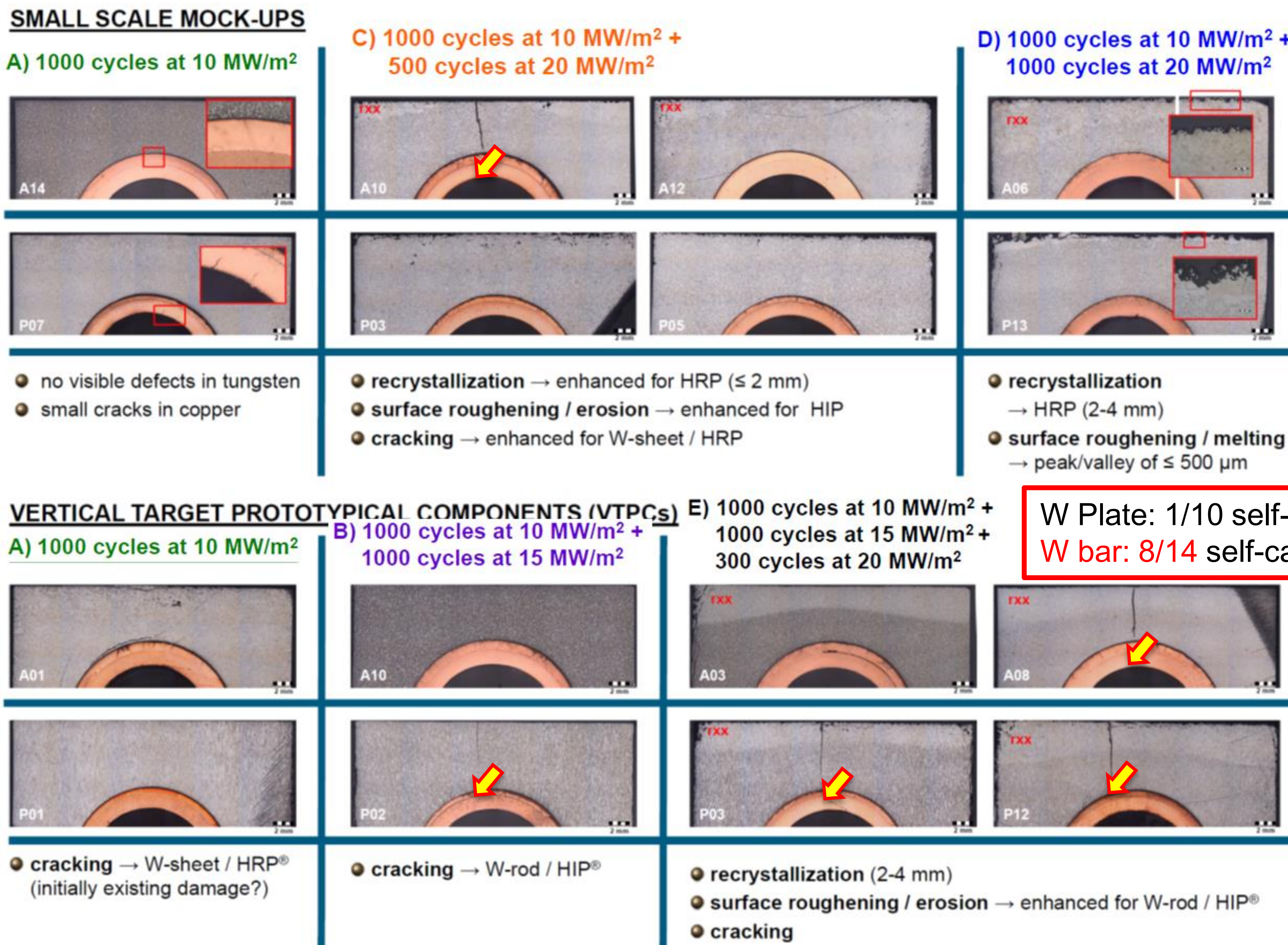

W Plate: 1/10 self-castellation
W bar: 8/14 self-castellation

G. Pintsuk, et al. “Qualification and post-mortem characterization of tungsten mock-ups exposed to cyclic high heat flux loading”, SOFT2012 Liege BE

Difference in W Materials

- Observation
  - Self-castellation often appeared in W monoblocks used by EU industry
- Conformity of W material with ITER material specification
  - Chemical composition: similar
  - Hardness: similar
  - Density: similar

	W-Plansee	W-Polema	W-ALMT	W-AT&M
HV30	441	443	461	448
density [g/cm^3]	19.25	19.12	19.17	19.25

  - Microstructure: different

    N.B. production routes are different (e.g. forged bar vs rolled plates)

Forged bar

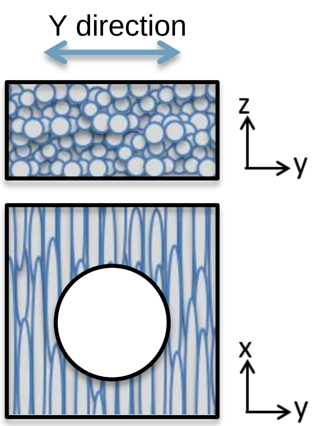

Rolled plate

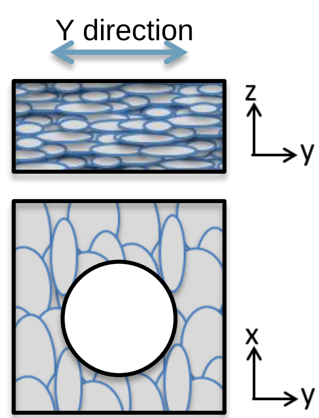

Strength in y-direction would be different

See supporting data in M. Wirtz, et al. presented at SOFT2012 http://dx.doi.org/10.1016/j.fusengdes.2013.05.07

Required Tests and Examinations

- Recrystallization Sensitivity Tests
  - Heat treatment at 1300 °C, 1500 °C, 1800 °C for 1 hour in vacuum
  - Test surface yz-plane
  - Vickers hardness HV30, microstructure and grain size

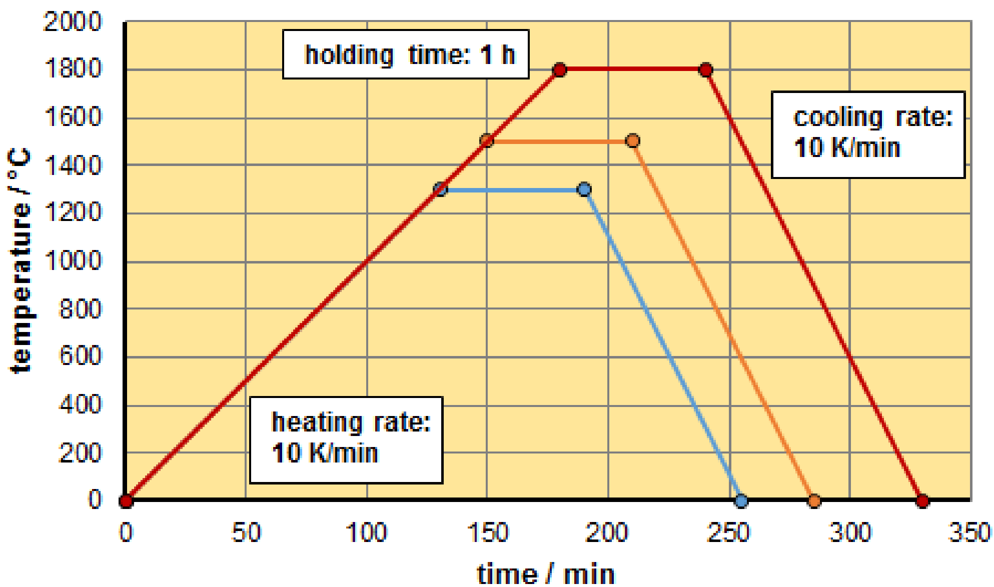

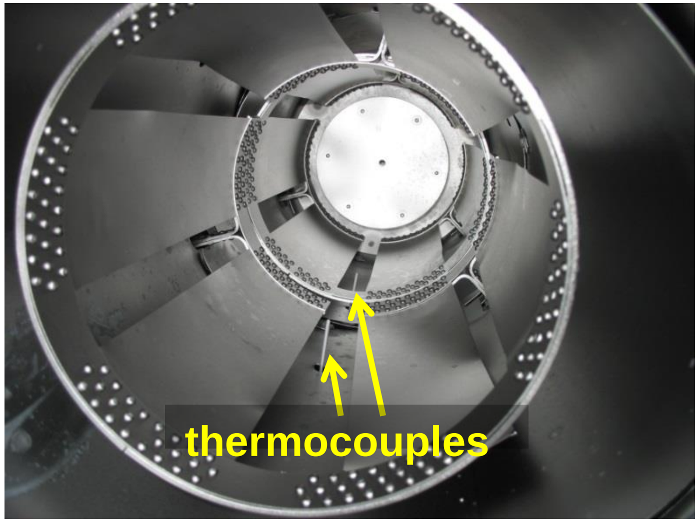

Temperature profiles up to 1300, 1500 and 1800 °C for the annealing treatment of the tungsten products

High temperature furnace with the position of the thermocouples.

Hardness Measurements

Vickers Hardness HV30

tested surface xy-plane

temperature treatment for 1 h

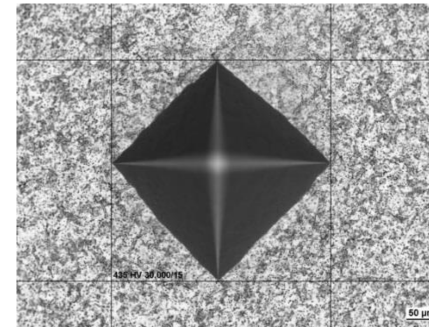

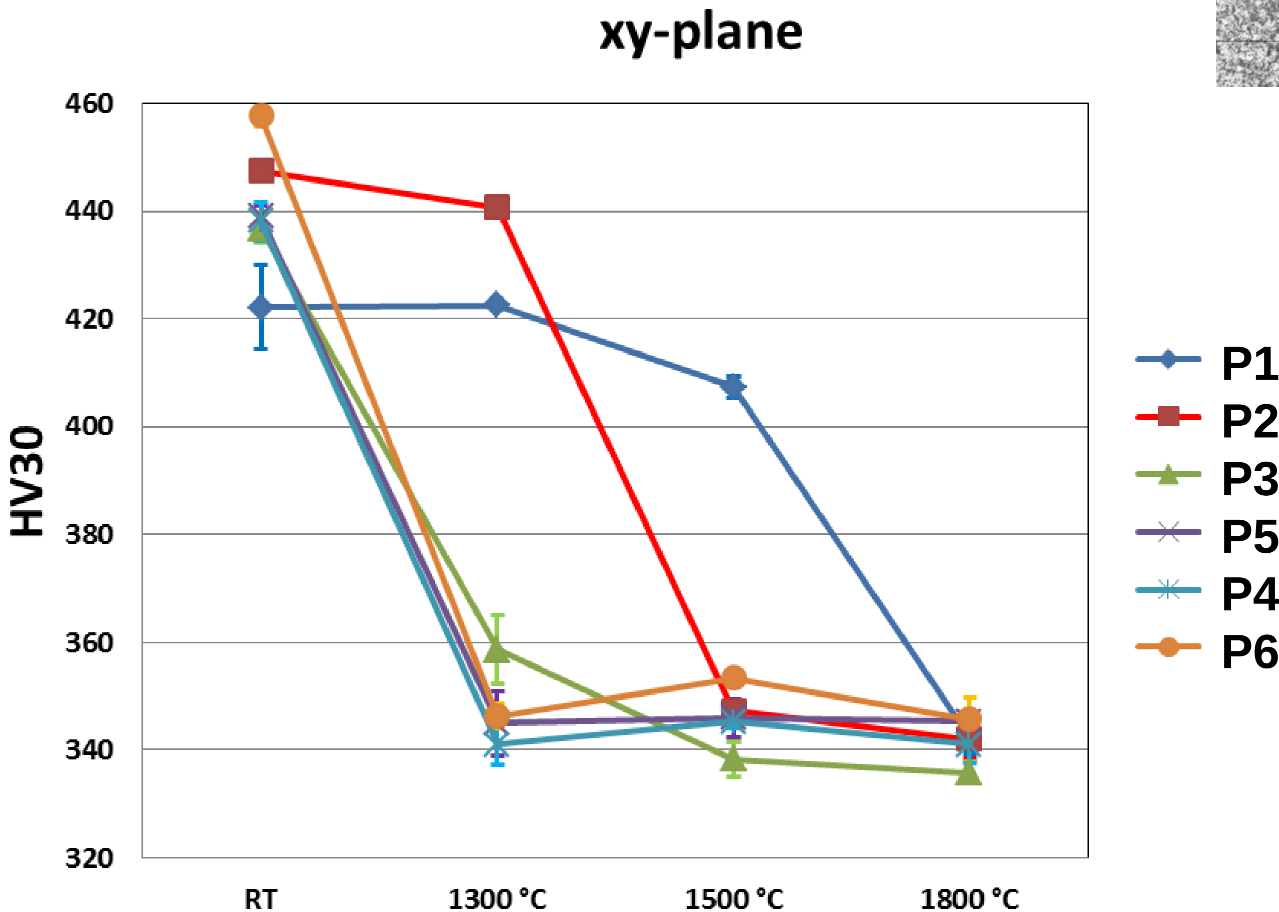

Hardness Measurements

Vickers Hardness HV30

tested surface yz-plane

temperature treatment for 1 h

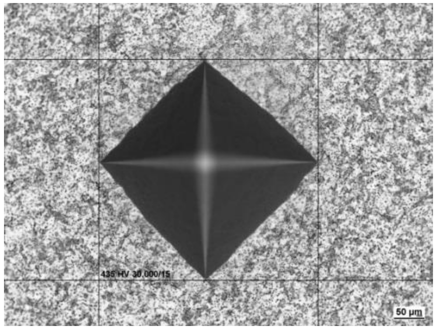

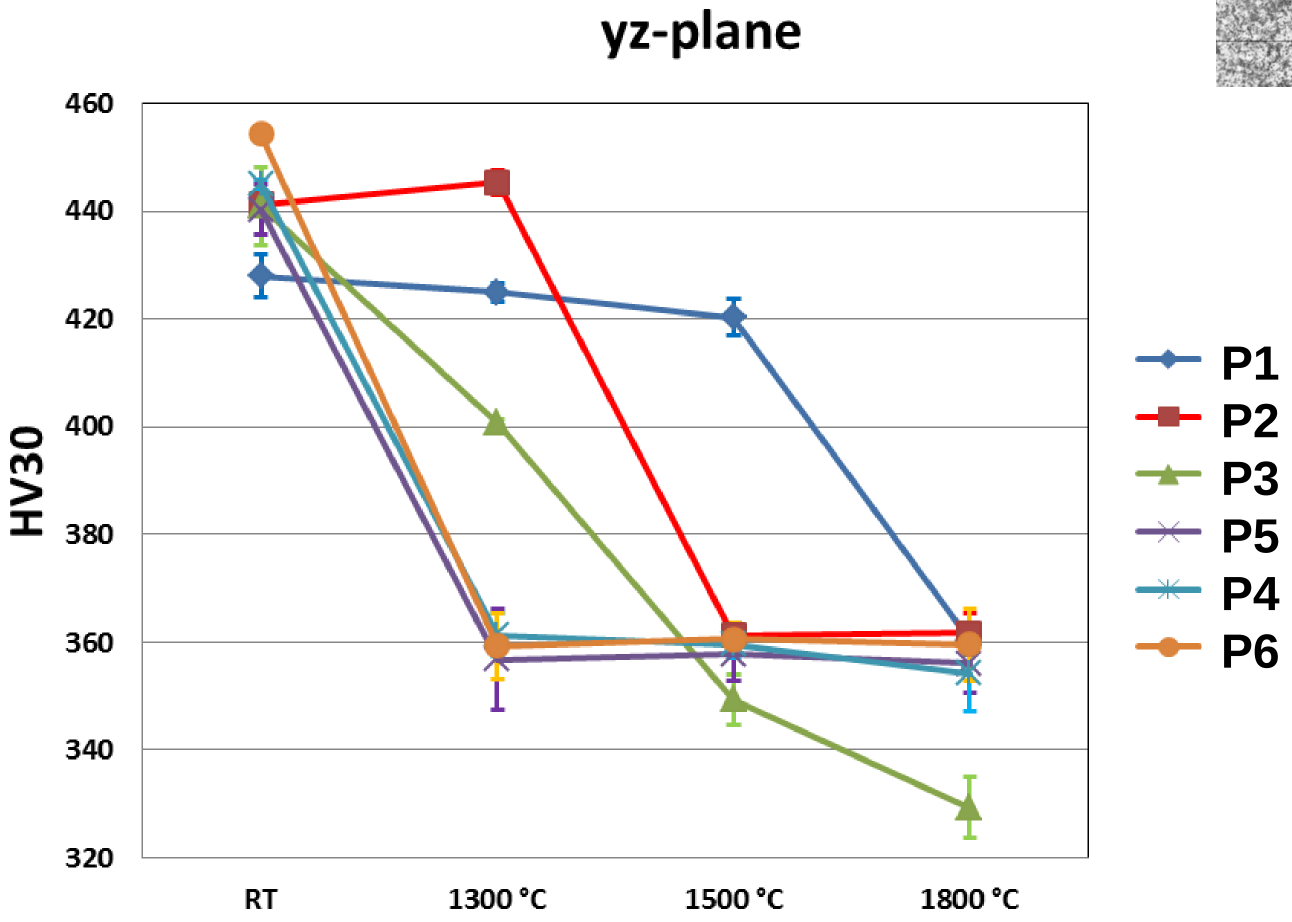

Hardness Measurements

Hardness difference of the xy and yz-plane

temperature treatment for 1 h

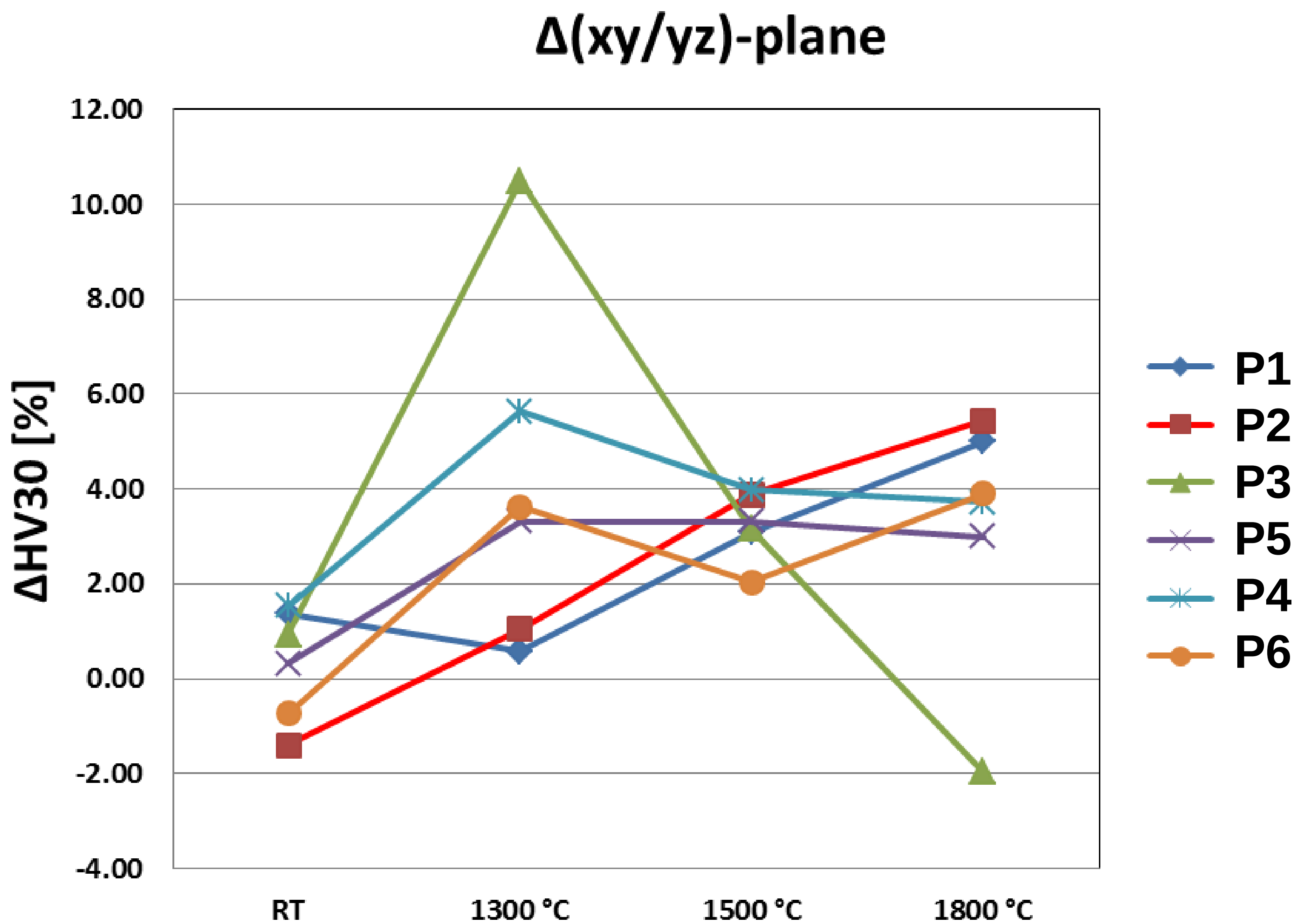

Microstructural observation

Investigated surface xy-plane

RT

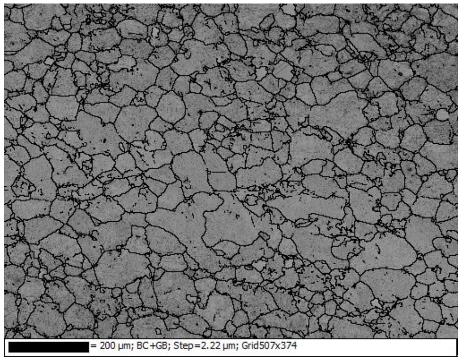

1800 °C

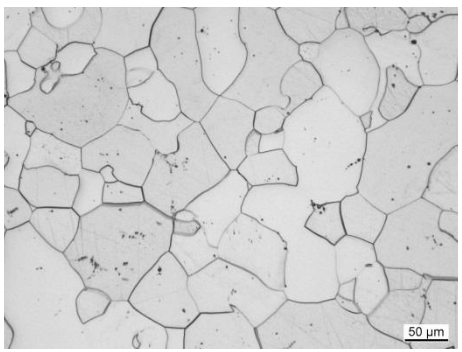

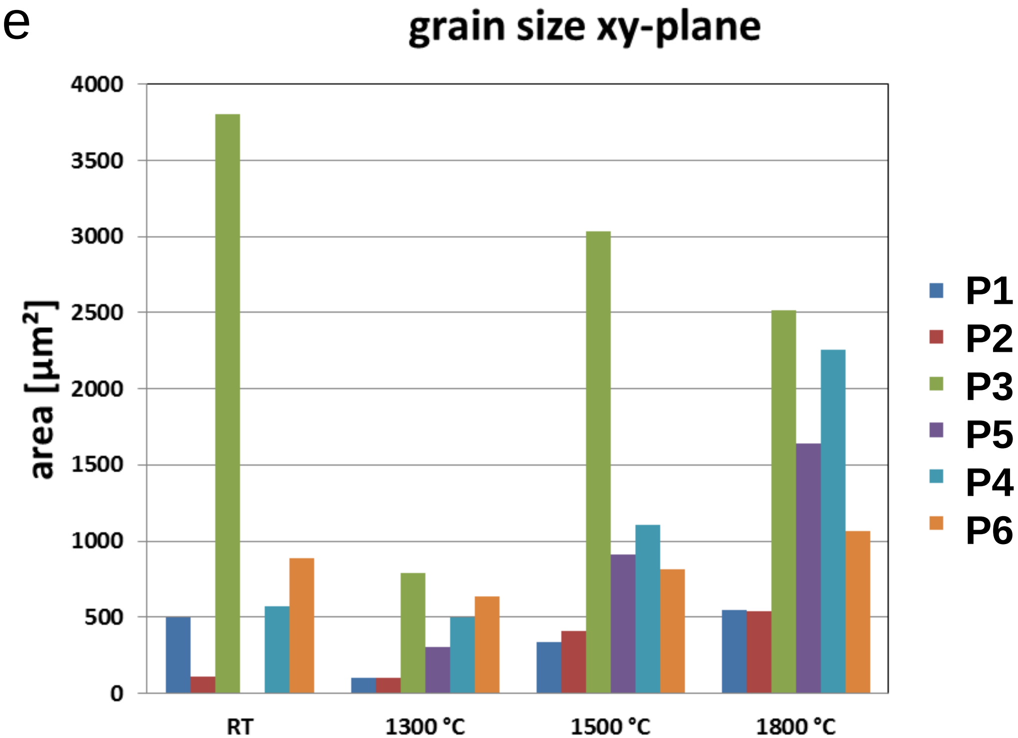

aspect ratio	ALMT	Ansaldo Polema	AT&M	Plansee (M213)	MMC NSMC	STARCK
RT	0.63	0.59	0.61	-	0.62	0.53
1300 °C	0.53	0.53	0.62	0.59	0.59	0.67
1500 °C	0.66	0.61	0.55	0.59	0.63	0.62
1800 °C	0.55	0.66	0.61	0.60	0.63	0.65

Microstructural observation

Investigated surface yz-plane

RT

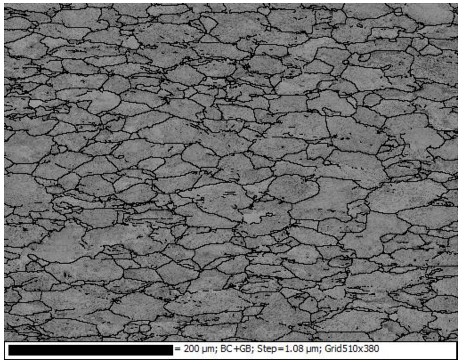

1800 °C

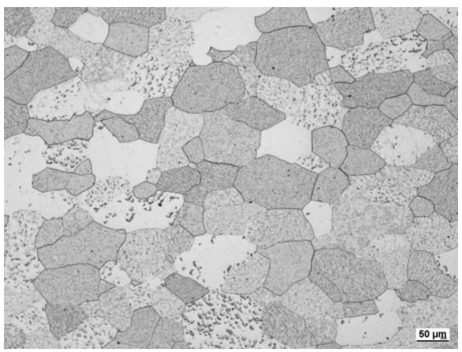

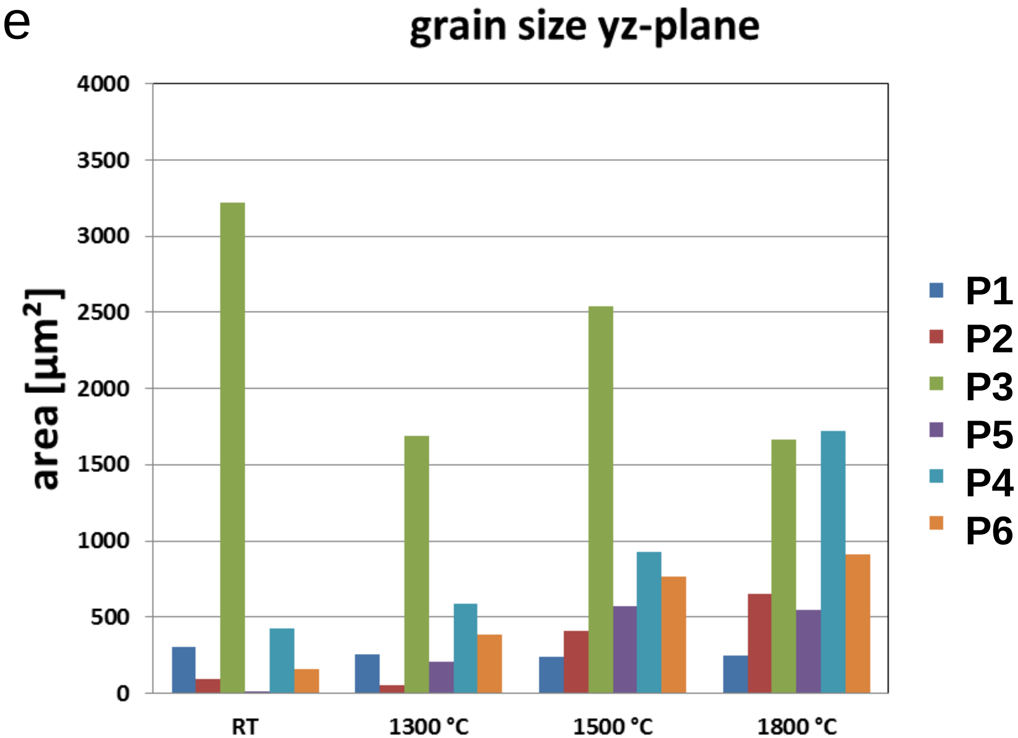

aspect ratio	ALMT	Ansaldo	AT&M	Plansee (M213)	MMC NSMC	STARCK
RT	0.50	0.47	0.48	0.50	0.36	0.27
1300 °C	0.50	0.43	0.53	0.65	0.49	0.61
1500 °C	0.56	0.69	0.60	0.59	0.57	0.60
1800 °C	0.54	0.70	0.53	0.64	0.64	0.61

Summary & Outlook

- Extensive characterization of the thermal shock behavior of W (interaction between material properties and damage behavior)
- Synergistic effects of particle and transient heat loads on thermal shock performance of W (H/He embrittlement, microstructural changes)
- Development of advanced tungsten materials with improved micro-structure
- Characterization of commercially available and new developed W grades

- Selection of W reference materials/samples for n-irradiation
- Thermal shock exposure of W reference materials after n-irradiation/comparison with un-irradiated damage response
- Thermal shock exposure of new developed W grades (e.g. PIM, Wf/W)
- Synergistic effects of particle and transient heat loads on thermal shock performance of reference W and new developed W grades after n-irradiation
- Characterization of the thermal and mechanical properties after n-irradiation